



**HAL**  
open science

## Rapid and extensive uptake and activation of hydrophobic triphenylphosphonium cations within cells

Meredith F Ross, Tracy A Prime, Irina Abakumova, Andrew M James, Carolyn M Porteous, Robin Aj Smith, Michael P Murphy

► **To cite this version:**

Meredith F Ross, Tracy A Prime, Irina Abakumova, Andrew M James, Carolyn M Porteous, et al.. Rapid and extensive uptake and activation of hydrophobic triphenylphosphonium cations within cells. Biochemical Journal, 2008, 411 (3), pp.633-645. 10.1042/BJ20080063 . hal-00478949

**HAL Id: hal-00478949**

**<https://hal.science/hal-00478949>**

Submitted on 30 Apr 2010

**HAL** is a multi-disciplinary open access archive for the deposit and dissemination of scientific research documents, whether they are published or not. The documents may come from teaching and research institutions in France or abroad, or from public or private research centers.

L'archive ouverte pluridisciplinaire **HAL**, est destinée au dépôt et à la diffusion de documents scientifiques de niveau recherche, publiés ou non, émanant des établissements d'enseignement et de recherche français ou étrangers, des laboratoires publics ou privés.

## Rapid and extensive uptake and activation of hydrophobic triphenylphosphonium cations within cells

Meredith F. ROSS\*, Tracy A. PRIME\*, Irina ABAKUMOVA\*, Andrew M. JAMES\*, Carolyn M. PORTEOUS§, Robin A. J. SMITH† and Michael P. MURPHY\*<sup>1</sup>

\*Medical Research Council Dunn Human Nutrition Unit, Wellcome Trust/MRC Building, Hills Road, Cambridge CB2 0XY, UK and the Departments of §Biochemistry and †Chemistry, University of Otago, PO Box 56, Dunedin, New Zealand.

<sup>1</sup>To whom correspondence should be addressed: Dr Michael P. Murphy, Medical Research Council Dunn Human Nutrition Unit, Wellcome Trust/MRC Building, Hills Road, Cambridge CB2 0XY, United Kingdom. Tel: +441223 252 900. Fax: +441223 252 905. E-mail: [mpp@mrc-dunn.cam.ac.uk](mailto:mpp@mrc-dunn.cam.ac.uk).

Running title: Uptake of MitoQ by cells

Abbreviations used: ACN, acetonitrile; ACR, accumulation ratio; CoQ, coenzyme Q;  $\Delta\psi_m$ , mitochondrial membrane potential;  $\Delta\psi_p$ , plasma membrane potential; ESI-MS, electrospray ionization mass spectrometry; FCCP, carbonylcyanide *p*-(trifluoromethoxy)phenylhydrazone; FCS, fetal calf serum; IDTP, 10-iododecyltriphenylphosphonium iodide; MitoQ, MitoQuinone; MitoQH<sub>2</sub>, MitoQuinol; PBS, phosphate buffered saline; PMPI, Plasma Membrane Potential Indicator; ROS, reactive oxygen species; TFA, trifluoroacetic acid; TMA-OH, tetramethylammonium hydroxide; TPB, tetraphenylborate; TPMP, methyltriphenylphosphonium; TPP, triphenylphosphonium cation.

### Abstract

Mitochondria-targeted molecules comprising the lipophilic triphenylphosphonium (TPP) cation covalently linked to a hydrophobic bioactive moiety are used to modify and probe mitochondria in cells and *in vivo*. However it is unclear how hydrophobicity affects the rate and extent of their uptake into mitochondria within cells, making it difficult to interpret experiments because their intracellular concentrations in different compartments are uncertain. To address this issue, we compared the uptake into isolated mitochondria, and mitochondria within cells, of two hydrophobic TPP derivatives, [<sup>3</sup>H]-MitoQ and [<sup>3</sup>H]-DecylTPP, with the more hydrophilic TPP cation [<sup>3</sup>H]-TPMP. Uptake of MitoQ by mitochondria and cells was described by the Nernst equation and was ~5-fold greater than that for TPMP, due to its greater binding within the mitochondrial matrix. DecylTPP was also taken up extensively by cells, indicating that increased hydrophobicity enhanced uptake. Both MitoQ and DecylTPP were taken up very rapidly into cells, coming to a steady state within 15 min, compared to ~8 h for TPMP. This far faster uptake was due to the increased rate of passage of hydrophobic TPP molecules through the plasma membrane. Within cells MitoQ was predominantly within mitochondria where it was rapidly reduced to the ubiquinol, consistent with its protective effects in cells and *in vivo* being due to the ubiquinol antioxidant. The strong influence of hydrophobicity on TPP cation uptake into mitochondria within cells facilitates the rational design of mitochondria-targeted compounds to report on and modify mitochondrial function *in vivo*.

Key words: mitochondria, lipophilic cations, MitoQ, membrane potential, mitochondrial targeting.

## INTRODUCTION

Mitochondria are central to many aspects of biomedical science; consequently there is considerable interest in the development of small molecules that can be targeted to mitochondria in cells and *in vivo* to report on and modify mitochondrial function [1]. Lipophilic cations such as triphenylphosphonium (TPP) have been linked covalently to small molecule thiol probes, spin traps, peptide nucleic acid oligomers, superoxide probes and antioxidants to deliver them to mitochondria, driven by the mitochondrial membrane potential ( $\Delta\psi_m$ ) [2-13]. The delocalised positive charge on the lipophilic TPP cation promotes their  $\Delta\psi_m$ -dependent accumulation into mitochondria and their direct passage through phospholipid bilayers, consequently these molecules are useful in a range of mitochondrial studies [1, 14].

Mitochondrial oxidative damage contributes to many pathologies because mitochondria are a source of reactive oxygen species (ROS) and are also susceptible to oxidative damage [15, 16]. To prevent oxidative damage, mitochondria-targeted antioxidants have been developed [17-19]. The prototypical mitochondria-targeted antioxidant is MitoQ (Figure 1), which comprises a ubiquinone moiety linked covalently by an aliphatic ten-carbon chain to the TPP cation [13, 20, 21]. MitoQ protects cells in culture against oxidative damage [13, 17, 22], is taken up into organs following oral administration [19], protects against tissue damage in animal models of disease [18, 23, 24] and is now undergoing Phase II clinical trials [25].

The interaction of MitoQ with the mitochondrial respiratory chain in simple systems is reasonably well understood. MitoQ is readily reduced to the ubiquinol form (MitoQH<sub>2</sub>) by complex II, but is a poor substrate for isolated complex I, isolated electron transfer flavoprotein-ubiquinone oxidoreductase and complex III [20, 21]. MitoQ adsorbs extensively to phospholipid bilayers, with its TPP moiety localised to a potential energy well near the membrane surface, while the chain allows access of the ubiquinone moiety to the membrane core and the active site of complex II [14, 20, 21]. In isolated mitochondria, MitoQ is rapidly taken up and converted to the ubiquinol form that prevents lipid peroxidation [13, 26]. However, little is known about the rate and extent of MitoQ uptake into mitochondria within cells and whether MitoQ is substantially reduced to its ubiquinol form.

Most mitochondria-targeted TPP probes are similar to MitoQ, therefore the rate and extent of their uptake into cells is also unknown. Basic questions remain, such as whether increasing hydrophobicity increases or decreases rate and extent of uptake relative to simple TPP cations such as methyltriphenylphosphonium (TPMP; Figure 1). The uptake of simple cations such as TPMP in response to a  $\Delta\psi$  is described by the Nernst equation whereby cation uptake increases 10-fold for every 61.5 mV at 37°C.

$$\Delta\psi \text{ (mV)} = 61.5 \log_{10} \frac{[\text{TPP cation}]_{in}}{[\text{TPP cation}]_{out}} \quad (1)$$

However, it is unclear if the significant potential-independent binding to membranes of hydrophobic TPP cations causes deviations from Nernstian behavior [13]. These uncertainties hamper interpretation of data obtained using TPP molecules and restrict the rational development of further mitochondria-targeted compounds. Here we report on the uptake of the hydrophobic TPP cations MitoQ and DecylTPP (Figure 1) into mitochondria and cells and compare these with TPMP, a simple, hydrophilic TPP cation. We found that the uptake of hydrophobic TPP cations into mitochondria is described by the Nernst equation and that their uptake into cells is more extensive and rapid than TPMP. These findings facilitate

interpretation of experiments using mitochondria-targeted molecules and indicate how these compounds can be modulated rationally to optimize their properties.

## EXPERIMENTAL

### Synthesis and purification of radiochemicals

To synthesize [<sup>3</sup>H]-MitoQ a solution of idebenol mesylate (900 mg, 2.15 mmol) [27] was prepared by reacting idebenone with methane sulfonyl chloride and triethylamine followed by catalytic hydrogenation. This was added to CH<sub>2</sub>Cl<sub>2</sub> (5 mL) in a Nalgene tube which contained [<sup>3</sup>H]-triphenylphosphine [28] (220 mg, 0.84 mmol, 19.3 mCi), stirred to give an homogeneous solution and then evaporated under a nitrogen flow at 40°C. The tube was flushed with argon, sealed and stirred for 29 h at ~85°C. The tube was then cooled and the contents dissolved in CH<sub>2</sub>Cl<sub>2</sub> (~2 mL) and stirred vigorously while CH<sub>3</sub>COOC<sub>2</sub>H<sub>5</sub> was added in three portions (2, 3 and 5 mL) to precipitate the product. The mixture was stirred for ~5 min and then the CH<sub>2</sub>Cl<sub>2</sub> was evaporated by bubbling with nitrogen for 15 min. Once the solution volume was less than 10 mL, the mixture was allowed to settle for 10 min. The CH<sub>3</sub>COOC<sub>2</sub>H<sub>5</sub> layer was decanted, the semi-solid residue dissolved in CH<sub>2</sub>Cl<sub>2</sub> (~2 mL) and precipitated with CH<sub>3</sub>COOC<sub>2</sub>H<sub>5</sub> (10 mL) as before. This precipitation process was repeated once more. After the CH<sub>3</sub>COOC<sub>2</sub>H<sub>5</sub> layer was decanted, the remaining solvent was removed by a nitrogen stream to give mitoquinol mesylate as a white powder (380 mg, 66%, 10.3 mCi). Oxygen gas was then bubbled through a solution of tritiated mitoquinol mesylate (200 mg, 0.29 mmol) in 1:2 H<sub>2</sub>O/CH<sub>3</sub>CN (5 mL) for 30 min. The solution was then stirred in air for ~3 days at room temperature. The solution was evaporated under nitrogen at ~30°C to ~5 mL. H<sub>2</sub>O (~3 mL) was added and it was then freeze-dried to give a sticky orange solid (~200 mg). Column chromatography on silica gel (5 g) and elution with acetonitrile gave mitoquinone mesylate (118 mg, 0.17 mmol, 60% yield, 93% radiopurity by HPLC). All [<sup>3</sup>H]-MitoQ preparations were further HPLC-purified to >97% radiopurity, as described below, before use in experiments.

To synthesize [<sup>3</sup>H]-DecylITPP a solution of 1-bromodecane (5.49 mg, 24.8 μmol) in N,N-dimethylformamide (13 μL) was added to [<sup>3</sup>H]-triphenylphosphine [28] (1.3 mg, 5 μmol, 11.9 μCi) in a 300 μL reaction vial. The solution was sparged with argon, stirred at 120°C for 24 h, allowed to cool to room temperature and the residue dissolved in minimum CH<sub>2</sub>Cl<sub>2</sub> (~60 μL) and transferred to a pre-weighed 2.5 mL screw cap glass vial. Addition of C<sub>2</sub>H<sub>5</sub>OC<sub>2</sub>H<sub>5</sub> (2 mL) gave a precipitate and the tube was then centrifuged at 600 x g for 10 min and the supernatant decanted. The residue was re-dissolved in minimum CH<sub>2</sub>Cl<sub>2</sub> and precipitated with C<sub>2</sub>H<sub>5</sub>OC<sub>2</sub>H<sub>5</sub> again. This process was repeated a total of four times. The final solid (~1 mg, 0.58 μCi) was dried under a stream of nitrogen.

[<sup>3</sup>H]-MitoQ, [<sup>3</sup>H]-DecylITPP and [<sup>3</sup>H]-TPMP iodide (60 Ci/mmol, from American Radiolabeled Chemicals) were further purified before use by RP-HPLC. [<sup>3</sup>H]-MitoQ (<100 nmol; 10–20 Ci/mol) was loaded in 1 mL 45% acetonitrile/0.1% TFA onto a C18 column (Jupiter 5 μm 300 Å, 250 x 4.6 mm, Phenomenex) and was eluted using a gradient of acetonitrile/0.1% TFA (4.5–54% over 5 min, then 54–72% over 20 min) at 1 mL/min. The A<sub>220</sub> of the column eluant was detected using a Gilson UV/VIS 151 spectrophotometer, and 0.5 mL fractions were collected around the [<sup>3</sup>H]-MitoQ peak, transferred to scintillation vials containing 3 mL Fluoransafe (BDH) and the radioactivity quantified using a Packard Tri-Carb 2800TR liquid scintillation analyser with appropriate quench corrections. Radioactive MitoQ fractions were pooled, lyophilized, resuspended in ethanol at 0.5–2 mM, and stored at –20°C. Radiopurity was determined by RP-HPLC as above by comparing the radioactivity of product fractions with 0.5 mL fractions collected over the entire gradient. Greater than 97%

of eluted radioactivity co-eluted with MitoQ, with less than 0.2% in any other fraction. The specific activity of [<sup>3</sup>H]-MitoQ was determined within each sample by counting of 2 x 200  $\mu$ L of suspension immediately after addition of [<sup>3</sup>H]-MitoQ. [<sup>3</sup>H]-DecylITPP and [<sup>3</sup>H]-TPMP were purified in the same way.

### Synthesis of 10-iododecyltriphenylphosphonium iodide (IDTP)

1,10-Diiododecane (2.4 g, 6.1 mmol) and triphenylphosphine (0.262 g, 1 mmol) were stirred in a Kimax tube at 75–80°C overnight. The tube was cooled, the reaction dissolved in minimum  $\text{CH}_2\text{Cl}_2$  (4 mL) and added dropwise to  $\text{C}_2\text{H}_5\text{OC}_2\text{H}_5$  (100 mL). The crude product was isolated by filtration and purified by silica gel chromatography. Elution with 1:1 acetonitrile/ $\text{CH}_2\text{Cl}_2$  and acetonitrile gave a product (0.559 g, 0.85 mmol, 85%) that was 97.6% pure as judged by HPLC. <sup>1</sup>H NMR  $\delta$  7.67–7.87 (m, 15 H,  $\text{PPh}_3$ ), 3.74 (m, 2 H,  $-\text{CH}_2\text{PPh}_3$ ), 3.171 (t, 2 H, 7 Hz,  $-\text{CH}_2\text{I}$ ), 1.52–1.83 (m, 6 H), 1.18–1.39 (m, 10 H) ppm. <sup>31</sup>P NMR  $\delta$  25.57 ppm. (+)ESI-MS found 529.153 ( $\text{C}_{28}\text{H}_{35}\text{PI}^+$  requires 529.152).

### Uptake of [<sup>3</sup>H]-MitoQ by isolated mitochondria.

Rat liver mitochondria were prepared by homogenization followed by differential centrifugation at 4°C in 250 mM sucrose, 5 mM HEPES, and 1 mM EGTA, pH 7.2 [29]. For the <sup>86</sup>Rb<sup>+</sup> uptake experiments buffer pH was adjusted using tetramethylammonium hydroxide (TMA-OH) in place of KOH. The protein concentration was determined by the biuret assay using BSA as a standard [30].

The simultaneous accumulation of <sup>86</sup>Rb<sup>+</sup> and [<sup>3</sup>H]-MitoQ or [<sup>3</sup>H]-TPMP was measured as described [31]. Briefly, mitochondria (2 mg protein.mL<sup>-1</sup>) were incubated for 5 min at 30°C in 250  $\mu$ L of 250 mM sucrose, 5 mM HEPES, 1 mM EGTA, pH 7.2 (TMA-OH) supplemented with 4  $\mu$ g.mL<sup>-1</sup> rotenone, 0.2 nmol valinomycin.mg protein<sup>-1</sup>, 10 mM succinate (TMA salt), <sup>86</sup>RbCl (5 nCi.mL<sup>-1</sup>) and 1  $\mu$ M [<sup>3</sup>H]-MitoQ or [<sup>3</sup>H]-TPMP (3–10 nCi.mL<sup>-1</sup>). The membrane potential was varied by addition of KCl (0–20 mM)  $\pm$  carbonylcyanide *p*-trifluoromethoxyphenylhydrazone (FCCP; 0.5  $\mu$ M). Experiments to determine mitochondrial binding in the absence of  $\Delta\psi_m$  were carried out in the presence of 0.5  $\mu$ M FCCP/20 mM KCl, and 0.3–1  $\mu$ M [<sup>3</sup>H]-MitoQ. After incubation mitochondria were pelleted by centrifugation, and 400  $\mu$ L supernatant and pellet <sup>3</sup>H and <sup>86</sup>Rb content assayed [31]. In parallel experiments the non-mitochondrial sucrose space in the pellets was determined by incubation with [<sup>14</sup>C]sucrose (50 nCi.mL<sup>-1</sup>) and was used to correct the apparent pellet spaces for non-mitochondrial <sup>86</sup>Rb<sup>+</sup> or <sup>3</sup>H. These values were then divided by the mitochondrial volume under these conditions (0.6  $\mu$ L.mg protein<sup>-1</sup>) to give the accumulation ratio (ACR) [32].

$$ACR = \frac{\left[ \left( \frac{400 \cdot DPM_{\text{pellet}}}{DPM_{\text{supernatant}}} \right) - \text{sucrose space } (\mu\text{L} \cdot \text{mg protein}^{-1}) \right]}{\text{mitochondrial volume } (\mu\text{L} \cdot \text{mg protein}^{-1})} \quad (2)$$

### Cell culture and incubations

Cells were cultured at 37°C under humidified 95% air/5% CO<sub>2</sub>, in medium supplemented with penicillin (100 U.mL<sup>-1</sup>) and streptomycin (100  $\mu$ g.mL<sup>-1</sup>). The Jurkat human T lymphocyte cell line was grown in suspension in RPMI medium (Invitrogen) supplemented with 10% fetal calf serum (FCS), and cells were routinely maintained at densities of 0.2–2 x

$10^6$  cells.mL<sup>-1</sup>. C2C12 cells (mouse myoblast; ECACC) were maintained at subconfluence in Dulbecco's modified Eagle medium (DMEM; Invitrogen) supplemented with 10% FCS.

To test the acute toxicity of MitoQ Jurkat cells were seeded at  $1 \times 10^6$ .mL<sup>-1</sup> (2 mL) in six-well plates, and incubated with vehicle (DMSO, 0.1% v/v) or mitochondria-targeted compound (0–50  $\mu$ M) for 24 h. Cell integrity was measured by propidium iodide exclusion [33]. MitoQ and DecylTPP began to affect Jurkat cell viability at 1–2  $\mu$ M, therefore concentrations of 0.5  $\mu$ M were used for most experiments. For uptake studies cells were seeded at  $3 \times 10^6$ .mL<sup>-1</sup> and supplemented with 500 nM [<sup>3</sup>H]-MitoQ, [<sup>3</sup>H]-DecylTPP or [<sup>3</sup>H]-TPMP,  $\pm$  FCCP (5  $\mu$ M), oligomycin/myxothiazol (2  $\mu$ M of each; to abolish  $\Delta\psi_m$  selectively) or oligomycin (2  $\mu$ M)/myxothiazol (2  $\mu$ M)/gramicidin (10  $\mu$ g.mL<sup>-1</sup>) (to abolish both plasma membrane potential ( $\Delta\psi_p$ ) and  $\Delta\psi_m$ ). All additions were from stocks in DMSO or ethanol, and the final DMSO or ethanol in all incubations was  $\leq$  0.2% (v/v). For oligomycin/myxothiazol  $\pm$  gramicidin incubations, cells were incubated with the inhibitors for 30 min before addition of MitoQ. Cell density was measured in parallel incubations containing 500 nM unlabelled MitoQ, and showed negligible cell growth over the incubations shown, therefore cell density at  $t = 0$  was applied at all time points to calculate cellular uptake. Samples (1 mL) were taken at various time points and cells were pelleted by centrifugation (16000  $\times$  g for 1 min). Cell uptake was quantified as described [31]. The amount of [<sup>3</sup>H]-MitoQ in the pellet was expressed in pmol per million cells, or as an accumulation ratio, calculated assuming a water volume of 0.2 pL for a Jurkat cell [34].

#### Measurement of plasma membrane potential

Jurkat cells ( $3 \times 10^6$ /mL) in Dulbecco's PBS supplemented with CaCl<sub>2</sub> and MgCl<sub>2</sub>, glucose (25 mM) and FCS (0.5%) were incubated for 1 h at 37°C with the proprietary Plasma Membrane Potential Indicator (PMPI; a component of the FLIPR Membrane Potential Assay Kit, Explorer format – blue; Molecular Devices), added to 0.5  $\mu$ L.mL<sup>-1</sup> from a stock solution reconstituted according to the manufacturer's instructions. PMPI fluorescence in stirred cell suspensions in a 3 mL cuvette was detected over time in a Shimadzu RF 5301-PC fluorimeter ( $\lambda_{ex} = 542$  nm, slit width 3 nm;  $\lambda_{em} = 553$  nm, slit width 5 nm), and the effect of adding oligomycin, myxothiazol (both 5  $\mu$ M) and gramicidin (10  $\mu$ g.mL<sup>-1</sup>) was measured.

#### Extraction of MitoQ from cells and mitochondria

To determine the redox state of [<sup>3</sup>H]-MitoQ in cells, Jurkat cells ( $3 \times 10^6$  cells/mL) were incubated in 6 mL of medium supplemented with 500 nM [<sup>3</sup>H]-MitoQ. Where the effect of respiratory inhibitors was tested, cells were incubated with inhibitors or vehicle (ethanol 0.2% v/v) for 30 min prior to [<sup>3</sup>H]-MitoQ addition. Aliquots (4 mL) of the cell suspension were then transferred to two 2 mL Eppendorf tubes and pelleted by centrifugation (16000  $\times$  g for 1 min). The supernatant was aspirated, pellets were briefly centrifuged (10 s), and residual supernatant removed with a piece of rolled-up tissue paper, then 250  $\mu$ L of 90% acetonitrile/0.1% TFA was added and the mix was immediately vortexed vigorously. Samples were centrifuged (16000  $\times$  g for 1 min) and 200  $\mu$ L supernatant removed to fresh tubes, pooling within samples to give a total of 400  $\mu$ L, which was then recentrifuged and samples (300  $\mu$ L) were snap-frozen on dry ice. For HPLC samples were diluted with 0.1% TFA to give 45% acetonitrile/0.1% TFA, and analyzed immediately by RP-HPLC. Fractions (0.25 mL) were collected over a window where both redox forms of MitoQ eluted. MitoQuinol (MitoQH<sub>2</sub>) eluted at  $\sim$ 14.5 min/64% acetonitrile and MitoQuinone eluted at  $\sim$ 16.5 min/67% acetonitrile. Fractions were transferred to a scintillation vial containing 3 mL Fluoransafe scintillant and the radioactivity determined. To determine the redox state of MitoQ in the extracellular medium, 1 mL of the supernatant obtained after pelleting cells was

added to 1 mL acetonitrile/0.2% TFA, vortexed vigorously and centrifuged (16 000 x *g* for 5 min). Supernatant (1.96 mL) was removed to a fresh tube, centrifuged again and a sample (1.92 mL) analyzed immediately by RP-HPLC. Mock extractions of chemically reduced [<sup>3</sup>H]-MitoQH<sub>2</sub> added to cell pellets immediately after addition of 250 μL 90% acetonitrile/0.1% TFA showed negligible oxidation of [<sup>3</sup>H]-MitoQH<sub>2</sub> during extraction and freeze-thawing.

To determine the redox state of [<sup>3</sup>H]-MitoQ after incubation with mitochondria, rat liver mitochondria (250 μg protein.mL<sup>-1</sup>) were incubated in 250 mM sucrose, 5 mM HEPES, and 1 mM EGTA, pH 7.4 supplemented with 500 nM [<sup>3</sup>H]-MitoQ and with other substrates and inhibitors as indicated, for 5 min at 37°C. The mitochondria were then pelleted by centrifugation (16000 x *g* for 5 min) and the pellets were extracted as described for cells, except that all centrifugation steps were 1 min; under these conditions there was negligible oxidation of added [<sup>3</sup>H]-MitoQH<sub>2</sub> during extraction, but freeze-thawing caused some oxidation of [<sup>3</sup>H]-MitoQH<sub>2</sub>, so mitochondrial extracts were analyzed by HPLC immediately after extraction.

To identify metabolites of [<sup>3</sup>H]-MitoQ, cells (3 x 10<sup>6</sup>.mL<sup>-1</sup>) were incubated with 500 nM [<sup>3</sup>H]-MitoQ for up to 72 h, before pelleting the cells and extracting MitoQ and its metabolites from the pellet. RP-HPLC was done as above, except that 60 x 0.5 mL fractions were collected, spanning the initial flowthrough and the entire gradient. The radioactivity in each fraction was quantified by scintillation counting of 50 μL of the eluant. Any fractions other than [<sup>3</sup>H]-MitoQ and [<sup>3</sup>H]-MitoQH<sub>2</sub> that contained >5% of the total eluted radioactivity after 48 h incubation were noted, and the same fractions collected from a parallel cell incubation with nonradioactive MitoQ. These fractions were analyzed by ESI-MS by direct infusion into a 4000 QTrap LC/MS/MS (Applied Biosystems) in positive ion mode and analysis at 150°C, ion spray voltage 4500 V. Calibration was by polyethylene glycol. Data were analyzed using Analyst software.

### Measurement of serum binding of MitoQ and TPMP

Binding of [<sup>3</sup>H]-MitoQ or [<sup>3</sup>H]-TPMP to serum, which was present at 10% (v/v) for all cell incubations, were determined by equilibrium dialysis [35]. Two dialysis cassettes (Pierce; molecular weight cut-off 3500 Da) containing 2 mL 10% FCS/PBS were placed in 500 mL PBS supplemented with [<sup>3</sup>H]-MitoQ (specific activity 5.6 Ci/mol; 500 nM) or [<sup>3</sup>H]-TPMP (specific activity 10.4 Ci/mol; 200 nM), and incubated with stirring at 37°C for up to 48 h. Samples (500 μL) were taken from the PBS medium and from dialysis cassettes, mixed with 3 mL Fluoransafe scintillant and the radioactivity quantified and compared to determine the binding to serum. [<sup>3</sup>H]-MitoQ and [<sup>3</sup>H]-TPMP uptake into the dialysis cassettes stabilized within 48 h. At this time point, 78% of [<sup>3</sup>H]-MitoQ was bound to serum while there was negligible binding of [<sup>3</sup>H]-TPMP to serum.

### Confocal microscopy

Fibroblasts were grown to semi-confluence on 22 mm diameter glass cover slips in 6-well culture plates. Cells were incubated with IDTP (1 μM) for 3.5 h ± FCCP (5 μM). MitoTracker Orange (Molecular Probes; 25 nM) was added at 3 h. Immunocytochemistry was carried out as described [36], and cells were visualized on a Zeiss LSM 510 Meta inverted confocal microscope using a 63x objective, 488 and 543 nm laser lines and 515/30 and 560LP filter sets.

## RESULTS

### The uptake of MitoQ by mitochondria is described by the Nernst equation

Hydrophobic lipophilic cations such as MitoQ (Figure 1) are extensively internalized by mitochondria driven by the membrane potential ( $\Delta\psi_m$ ), but it is unclear if their significant potential-independent binding to membranes causes deviations from Nernstian behavior [13]. To address this we measured the uptake and binding of [ $^3\text{H}$ ]-MitoQ by isolated mitochondria over a range of  $\Delta\psi_m$  values while simultaneously measuring  $^{86}\text{Rb}^+$  uptake (Figure 2). In the presence of valinomycin  $^{86}\text{Rb}^+$  uptake is solely determined by  $\Delta\psi_m$  [32, 37]. Dual isotope counting enabled the apparent pellet spaces of  $^{86}\text{Rb}^+$  and [ $^3\text{H}$ ]-MitoQ to be determined simultaneously over a  $\Delta\psi_m$  range set by various amounts of KCl [31, 37]. From the known mitochondrial volume, and parallel measurement of the distribution of membrane-impermeant [ $^{14}\text{C}$ ]sucrose to calculate the non-mitochondrial pellet space, the accumulation ratios ( $= [\text{compound}]_{\text{mitochondria}}/[\text{compound}]_{\text{supernatant}}$ ) for [ $^3\text{H}$ ]-MitoQ and  $^{86}\text{Rb}^+$  were calculated [31]. Applying the Nernst equation to the  $^{86}\text{Rb}^+$  accumulation ratio enabled the MitoQ accumulation ratio to be plotted over a range of known  $\Delta\psi_m$  values.

In Figure 2A the accumulation ratio of the simple lipophilic cation [ $^3\text{H}$ ]-TPMP is plotted against that for  $^{86}\text{Rb}^+$  (lower x-axis) over a range of  $\Delta\psi_m$  values (upper x-axis). As expected, the relationship is linear up to the highest  $^{86}\text{Rb}^+$  accumulation ratio ( $\sim 900$ ,  $\Delta\psi_m \sim 174$  mV) indicating that [ $^3\text{H}$ ]-TPMP uptake is described by the Nernst equation. The slope is greater than unity because a fixed proportion of matrix TPMP is bound. A slope of  $\sim 2.1$  means that  $\sim 53\%$  of intramitochondrial TPMP is membrane-bound and the intercept with the y-axis close to the origin indicates that its binding to unenergized mitochondria is negligible [32, 37]. Plotting the [ $^3\text{H}$ ]-MitoQ accumulation ratio against that of  $^{86}\text{Rb}^+$  also gave a straight line (Figure 2B), but this line passed through the y-axis well above the origin (accumulation ratio  $\sim 8600$ ) due to substantial binding of [ $^3\text{H}$ ]-MitoQ to unenergized mitochondria (Figure 2B). The slope was 10.3 indicating that  $>90\%$  of intramitochondrial MitoQ is bound with  $<10\%$  free in the matrix. This is consistent with the greater hydrophobicity of MitoQ (the octan-1-ol:PBS partition coefficients for MitoQ and TPMP are  $\sim 3000$  and  $\sim 0.35$ , respectively [26]) and with its high affinity for phospholipid bilayers [20]. Thus, the  $\Delta\psi_m$ -dependent uptake of MitoQ by mitochondria is fully described by the Nernst equation.

To separate  $\Delta\psi_m$ -independent and -dependent binding we incubated unenergized mitochondria with  $0.3\text{--}1\ \mu\text{M}$  [ $^3\text{H}$ ]-MitoQ and measured free and bound [ $^3\text{H}$ ]-MitoQ, which gave a binding constant of  $5.1\ (\text{pmol}\cdot\text{mg protein}^{-1})\cdot\text{nM}^{-1}$  (Figure 2C). As the mitochondrial volume is  $0.6\ \mu\text{l}\cdot\text{mg protein}^{-1}$  this corresponds to an accumulation ratio of 8500 for uncoupled mitochondria, consistent with the intercept with the y-axis in Figure 2B. The TPMP binding constant was  $<1\%$  of that for MitoQ ( $\sim 0.038\ (\text{pmol}\cdot\text{mg protein}^{-1})\cdot\text{nM}^{-1}$ ) (Figure 2C). From this binding constant and the known free concentration of MitoQ we used the data from Figure 2B to calculate the  $\Delta\psi_m$ -independent mitochondrial binding of MitoQ, which was subtracted from the total accumulated to generate the  $\Delta\psi_m$ -dependent mitochondrial accumulation (Figure 2D). This plot was also a straight line of slope 10.3, further confirming that MitoQ uptake was Nernstian. Note that the y-axis intercept in Figure 2B depends solely on the free concentration of MitoQ and the mitochondrial amount, as described by Figure 2C, whereas the accumulation ratio-dependence on  $\Delta\psi_m$  is independent of [MitoQ].

From these data it was possible to model the  $\Delta\psi_m$ -dependent uptake of MitoQ and TPMP as a function of  $\Delta\psi_m$  at an external free concentration of  $10\ \text{nM}$  (Figure 2E), and as a function of external free concentration at  $\Delta\psi_m = 150\ \text{mV}$  (Figure 2F). These show that the  $\Delta\psi_m$ -dependent MitoQ uptake by mitochondria was always  $\sim 5$ -fold greater than that of TPMP, even though the Nernst equation predicts identical ratios of free MitoQ and TPMP

inside and outside mitochondria at a given  $\Delta\psi_m$ . This occurs because the greater binding of MitoQ within the mitochondrial matrix increases its  $\Delta\psi_m$ -dependent uptake. Therefore the  $\Delta\psi_m$ -dependent uptake of hydrophobic TPP compounds such as MitoQ is fully described by the Nernst equation and is greater than more hydrophilic TPP compounds.

### Rapid and extensive uptake of MitoQ and DecylTPP by cells

It was unknown if the greater hydrophobicity of TPP cations such as MitoQ increases or decreases the rate and extent of their uptake into cells compared to more hydrophilic cations such as TPMP. To address this we compared the uptake of MitoQ and DecylTPP with that of TPMP into Jurkat T lymphocytes. Use of a suspension cell line facilitates uptake studies because they can be rapidly isolated from the incubation medium by centrifugation [34]. We incubated cells with [ $^3\text{H}$ ]-MitoQ and isolated cells at various times over 24 h and measured the [ $^3\text{H}$ ]-MitoQ in the cell pellet and supernatant (Figure 3A). This experiment was repeated over a shorter time scale to show uptake over the first 40 min of incubation (Figure 3B). [ $^3\text{H}$ ]-MitoQ uptake into cells was rapid, with a steady state reached within  $\sim 12$  min and remaining stable for at least 24 h (Figs. 3A & B). In contrast, uptake of TPMP was slow, taking  $\sim 6$ –8 h to reach a steady state (Figure 3A,B). To see if these differences in uptake were due to hydrophobicity or were specific for the ubiquinone moiety of MitoQ, we measured the uptake of another hydrophobic TPP derivative DecylTPP, which lacks a ubiquinone (Figure 1). Uptake of DecylTPP was as rapid as that of MitoQ, quickly reaching a steady state (Figure 3B) and thereafter remaining stable (data not shown). Therefore increasing the hydrophobicity of TPP cations greatly increases their rate of uptake into cells.

To see if increasing the hydrophobicity of TPP cations also affected their efflux rate, we incubated cells with MitoQ or TPMP for 3 or 6 h, respectively, and then abolished  $\Delta\psi_m$  with FCCP and measured efflux over 90 min (Figure 3C). Efflux of MitoQ was rapid and was complete within 10 min, while efflux of TPMP took an hour (Figure 3C). Efflux showed first order kinetics, enabling rate constants and half lives ( $t_{1/2}$ ) to be calculated:  $k = 0.16 \text{ min}^{-1}$  and  $t_{1/2} \sim 4$  min for MitoQ;  $k = 0.03 \text{ min}^{-1}$  and  $t_{1/2} \sim 24$  min for TPMP (Figure 3C, inset). This 6-fold faster efflux of MitoQ compared with TPMP is consistent with the relative rates of cell uptake of the two compounds and suggests that the rate of movement of hydrophobic TPP compounds into and out of cells is significantly faster than for more hydrophilic compounds such as TPMP.

Substantially more MitoQ and DecylTPP were taken up by cells than TPMP (Figs. 3A & B). As the volume of Jurkat cells is  $\sim 0.2$  pL per cell [34] the uptake of compounds can be expressed as an accumulation ratio ( $\text{ACR} = [\text{TPP cation}]_{\text{cell}}/[\text{TPP cation}]_{\text{supernatant}}$ ) and for MitoQ the accumulation ratio was  $921 \pm 104$  at 3 h, 4.75-fold greater than that for TPMP ( $192 \pm 56$ ) (Figure 3D). When the uncoupler FCCP was added the accumulation ratios of MitoQ, DecylTPP and TPMP decreased by 81%, 87% and 79%, respectively (Figure 3D). These data are consistent with  $\Delta\psi_m$ -dependent uptake of all three TPP compounds into mitochondria after initial uptake into cells.

Therefore hydrophobic TPP compounds such as MitoQ and DecylTPP are more rapidly taken up into cells than the hydrophilic cation TPMP. These hydrophobic molecules are also 4–10 fold more extensively accumulated by cells than TPMP, consistent with their greater uptake into isolated mitochondria (Figure 2).

### Within cells hydrophobic TPP cations predominantly localize to mitochondria

FCCP led to the release of the TPP compounds from the cell, indicating that uptake of intracellular MitoQ, DecylTPP and TPMP is driven by  $\Delta\psi_m$  (Figure 3D). However, directly demonstrating the mitochondrial localization of TPP compounds within cells is challenging,

as they rapidly redistribute upon subcellular fractionation. To circumvent this, we investigated the uptake of a MitoQ analogue, IDTP (Figure 4). Like MitoQ and DecylTPP, IDTP contains the TPP targeting moiety and a ten-carbon aliphatic alkyl chain, but also has an iodo moiety that reacts slowly with protein thiols to form a stable thioether bond [11] (Figure 1). Thus the extent of covalent binding of IDTP to intracellular proteins is a reflection of its steady-state concentration within a cytosolic compartment. The TPP moiety of IDTP can be detected using anti-TPP antiserum enabling the localization of IDTP binding by immunocytochemistry [11]. IDTP was taken up rapidly into isolated mitochondria in a  $\Delta\psi_m$ -dependent manner, similar to MitoQ and DecylTPP (data not shown). In fibroblasts IDTP localized exclusively to mitochondria and this uptake was prevented by FCCP (Figure 4). In the C2C12 myoblast cell line IDTP localization was also mitochondrial and was prevented by FCCP and by oligomycin/myxothiazol (data not shown). The reactivity of protein thiols ( $pK_a$  typically 8–9) with IDTP within the mitochondrial matrix (pH ~8) is likely to be higher than in the cytosol (pH 7.2), because it is the thiolate form that reacts with IDTP [11]. However, there was negligible cytoplasmic IDTP binding in fibroblasts after 6 h incubation, suggesting that the steady state concentration of IDTP in the cytosol is far lower than in mitochondria. Together these data strongly suggest that within cells hydrophobic TPP compounds are predominantly concentrated within mitochondria driven by the  $\Delta\psi_m$ .

#### Cell uptake of MitoQ is consistent with the Nernst equation

The uptake of hydrophilic TPP cations such as TPMP into cells occurs in response to both the plasma membrane potential ( $\Delta\psi_p$ ) and the mitochondrial membrane potential ( $\Delta\psi_m$ ) as described by the Nernst equation [38, 39]. Uptake is determined experimentally as an accumulation ratio ( $ACR = [TPP\ cation]_{cell}/[TPP\ cation]_{supernatant}$ ) and this is related to  $\Delta\psi_p$  and  $\Delta\psi_m$  by equation 3 [38], where  $V_c$  and  $V_m$  are the volumes of the cytosol and mitochondria, and  $a_s$ ,  $a_c$  and  $a_m$  are the activity coefficients of the compounds in the extracellular environment, cytosol and the mitochondrial matrix, respectively (the activity coefficient is the proportion of compound in that compartment that is free in solution and not bound).

$$ACR = \frac{[TPP\ cation]_{Cell}}{[TPP\ cation]_{Supernatant}} = \frac{a_s \cdot 10^{\Delta\psi_p/61.5} \cdot \left\{ \frac{V_c}{a_c} + \frac{V_m}{a_m} \cdot 10^{\Delta\psi_m/61.5} \right\}}{V_c + V_m} \quad (3)$$

In Jurkat cells the plasma membrane potential is 40 mV (negative inside) [34] and the volume is 200 nL/10<sup>6</sup> cells with ~5% occupied by mitochondria [34], giving values for  $V_m$  and  $V_c$  of 10 nL/10<sup>6</sup> cells and 190 nL/10<sup>6</sup> cells, respectively. We determined that the serum binding of TPMP in these experiments was negligible, so  $a_s = 1$ . The cytoplasmic binding of TPMP within hepatocytes,  $a_c = 0.21$  [32], was taken as the value for  $a_c$  in Jurkat cells. The binding of TPMP within mitochondria, determined from the reciprocal of the slope of Figure 2A, gives  $a_m = 0.47$ . These parameters, together with the TPMP ACR of 192 from Figure 3D, give  $\Delta\psi_m = 157$  mV from equation 3, which is in the expected range [32]. Thus equation 3 describes the Nernstian uptake of TPP cations by cells in our experiments.

If the uptake of MitoQ into Jurkat cells is Nernstian then its ACR should also be described by equation 3. To assess this we require the activity coefficients of MitoQ in the three compartments. MitoQ was ~78% bound to serum in the incubation medium, consequently  $a_s = 0.22$ . The intramitochondrial binding of MitoQ, from the reciprocal of the slope in Figure 2B, indicates that  $a_m = 0.097$ . The extensive binding of MitoQ to deenergized cells makes it technically difficult to determine a reliable value for  $a_c$  [35]. This would

require abolishing  $\Delta\psi_p$  and  $\Delta\psi_m$  and comparing the [ $^3\text{H}$ ]-MitoQ ACR relative to that for  $^{86}\text{Rb}^+$  over a range of  $\Delta\psi_p$  values [35], as was done for mitochondria in Figure 2B. However for cells it is only possible to vary  $\Delta\psi_p$  over about 60 mV [35]. As can be seen in Figure 2B the extensive non-specific binding of MitoQ would render any  $\Delta\psi_p$ -sensitive uptake negligible relative to random errors in binding below  $\Delta\psi_p$  of  $\sim 120$  mV.

To determine  $a_c$  by an alternative approach we assume that equation 3 does describe MitoQ uptake, then we can use it to calculate  $a_c$ , from  $\Delta\psi_m = 157$  mV, the known values for  $V_m$ ,  $V_c$  and  $\Delta\psi_p$ , and the values of  $a_s$  and  $a_m$  that we have derived for MitoQ. Entering these values, along with the ACR for MitoQ of 921 from Figure 3D, gives  $a_c = 0.002$ . This indicates that our data on the uptake of MitoQ into cells are consistent with Nernstian uptake, provided  $\sim 99.8\%$  of the MitoQ in the cytosol is bound.

To check if this estimate for extensive ( $>99\%$ ) cytosolic binding of MitoQ was valid, we calculated  $a_c$  by an alternative method based on different starting assumptions. For the Jurkat cell incubation in Figure 3 the total [MitoQ] added was 500 nM which after equilibration reached a steady state total [MitoQ] in the extracellular medium of  $260 \pm 5$  nM (Figure 3D and data not shown). As  $\sim 78\%$  of extracellular MitoQ is bound to serum the free concentration is 57 nM. Assuming Nernstian uptake into the cytosol and mitochondria driven by a  $\Delta\psi_p$  of 40 mV and a  $\Delta\psi_m$  of 157 mV, the cytosolic and mitochondrial free MitoQ concentrations will be 255 nM and 91  $\mu\text{M}$ , respectively. From the cytosolic and mitochondrial volumes (190 nL and 10 nL/ $10^6$  cells) this gives 0.048 and 0.91 pmol MitoQ/ $10^6$  cells free in the cytosol and mitochondria, respectively. The total amount of cytosolic MitoQ can be estimated as that lost when cells incubated with myxothiazol and oligomycin to abolish  $\Delta\psi_m$  are further treated with gramicidin to abolish  $\Delta\psi_p$  (Figure 5C). The total amount of mitochondrial MitoQ can be estimated as that which is sensitive to abolishing  $\Delta\psi_m$  with myxothiazol and oligomycin (Figure 5A). From these experiments the total amounts of MitoQ present in the cytosolic and mitochondrial compartments are 16 pmol and 29.3 pmol MitoQ/ $10^6$  cells, respectively. Comparing these values with the free concentration of MitoQ estimated from the Nernst equation indicates that in the cytosolic free MitoQ is  $\sim 0.3\%$  of the total, with  $\sim 99.7\%$  bound. In mitochondria  $\sim 3\%$  of the total MitoQ is free with  $\sim 97\%$  bound. This estimate of  $\sim 99.7\%$  of cytosolic MitoQ bound is comparable to our earlier estimate of 99.8% bound, suggesting that  $a_c = 0.002$  for MitoQ is a reasonable estimate.

To summarize, uptake of MitoQ into cells is consistent with the Nernst equation, provided that binding of MitoQ in the cytosol is  $>99\%$ . It was not possible to determine directly MitoQ binding in the cytosol, but two different calculations suggest that cytosolic MitoQ is  $>99\%$  bound. MitoQ is far more hydrophobic than TPMP: octano-1-ol partition coefficients for MitoQ and TPMP are 2760 and 0.35, respectively [26]; affinity of MitoQ for unenergized mitochondrial membranes is 134-fold greater than that of TPMP (Figure 2C); and 78% of MitoQ was bound to serum in the incubation medium while binding of TPMP was negligible. In hepatocytes  $\sim 80\%$  of cytoplasmic TPMP is bound [32], making  $>99\%$  binding of the far more hydrophobic MitoQ plausible. Therefore our findings are consistent with uptake of MitoQ into cells being described by the Nernst equation with most intracellular compound being bound.

#### **Different rates of uptake of TPP cations across the plasma membrane**

The relatively hydrophobic TPP cations MitoQ and DecylTPP are far more rapidly taken up and released by cells than the hydrophilic TPMP cation (Figure 3). This discrepancy is not due to differences in rates of uptake into mitochondria as TPMP and MitoQ are both taken up

rapidly into isolated mitochondria with >90 % of uptake complete within 1 min [26, 28]. This suggests that the different uptake rates into cells are due to plasma membrane differences.

To measure the uptake of TPP compounds across the plasma membrane without the confounding effects of subsequent mitochondrial uptake, we abolished  $\Delta\psi_m$  with oligomycin and myxothiazol. While this loss of  $\Delta\psi_m$  decreased the extent of uptake of MitoQ (Figure 5A) and DecylTPP (data not shown), a steady state distribution was reached within 5 min (Figure 5A). Oligomycin and myxothiazol did not disrupt  $\Delta\psi_p$  over the time scale of these experiments, as measured by the fluorescent  $\Delta\psi_p$  indicator PMPI [40] (Figure 5B). Subsequent addition of the ionophore gramicidin collapsed  $\Delta\psi_p$  (Figure 5B) and further decreased uptake of MitoQ (Figure 5C) and DecylTPP (data not shown). Therefore the gramicidin-sensitive uptake of MitoQ and DecylTPP in the presence of myxothiazol and oligomycin is rapid and is primarily driven by  $\Delta\psi_p$ . In contrast, uptake of TPMP under these conditions was far slower than that of MitoQ or DecylTPP and was mostly prevented when  $\Delta\psi_p$  was abolished with gramicidin (Figure 5D). It is concluded that hydrophobic TPP compounds are taken up more rapidly into cells than TPMP because they cross the plasma membrane far more quickly.

### Redox state of MitoQ within mitochondria

The reduction of MitoQ to its ubiquinol form MitoQH<sub>2</sub> by the respiratory chain is thought to be essential for it to prevent lipid peroxidation [13, 41]. In simple *in vitro* systems, MitoQ is rapidly reduced by complex II, but in cells and isolated mitochondria little is known about the redox state of MitoQ or its rate of equilibration with endogenous electron donors. We therefore set out to investigate reduction of [<sup>3</sup>H]-MitoQ by mitochondria (Figure 6).

After incubation of mitochondria with [<sup>3</sup>H]-MitoQ, the ubiquinone ([<sup>3</sup>H]-MitoQ) and ubiquinol ([<sup>3</sup>H]-MitoQH<sub>2</sub>) forms were extracted into acidified acetonitrile, separated by HPLC, and quantitated by scintillation counting (Figure 6A). The ratio of the area under the [<sup>3</sup>H]-MitoQH<sub>2</sub> peak to the total amount recovered gave the percent reduction of MitoQ. Control experiments with exogenous [<sup>3</sup>H]-MitoQH<sub>2</sub> showed that this extraction and analysis procedure preserved the MitoQ redox state. In mitochondria energized with succinate, 75 ± 8% of [<sup>3</sup>H]-MitoQ was reduced (Figure 6B). Succinate-mediated reduction was largely abolished by the succinate dehydrogenase inhibitor malonate (17 ± 5% reduced), similar to the 24 ± 4% reduced found in the absence of exogenous substrate. In glutamate/malate-energized mitochondria, 61 ± 16% of MitoQ was reduced, and this was significantly decreased by rotenone (30 ± 3% reduced). FCCP abolished the  $\Delta\psi_m$ , thereby decreasing the amount of MitoQ associated with mitochondria (data not shown), but led to only a slight decrease in the extent of MitoQ reduction (Figure 6B).

As respiratory inhibitors abolish  $\Delta\psi_m$  they affect MitoQ uptake as well as inhibiting potential electron donors, complicating interpretation of their effects on MitoQ redox state. To overcome this we incubated mitochondria with MitoQ in the presence of FCCP, along with various inhibitors (Figure 6C). Under these conditions the complex III inhibitor myxothiazol further increased MitoQ reduction in succinate-energised mitochondria, and counteracted the inhibition of MitoQ reduction by malonate (Figure 6C). Similarly in glutamate/malate-energised mitochondria, myxothiazol also increased MitoQ reduction and counteracted inhibition of this reduction by rotenone (Figure 6C). As myxothiazol increases the level of reduction of the Coenzyme Q (CoQ) pool, these findings suggest that in mitochondria MitoQ becomes reduced in response to the redox state of the endogenous CoQ pool. Direct exchange between MitoQ and the endogenous CoQ pool is thermodynamically restricted in the low dielectric environment of the membrane [42], so the interaction between

MitoQ and the endogenous CoQ pool is most likely mediated through an enzyme active site. MitoQ is known to be a good substrate for complex II making it a good candidate for this reaction [20, 21]. However a contribution from complex I in the presence of the endogenous CoQ pool is also possible, even though the isolated complex is unreactive [21].

### Redox state and metabolism of MitoQ within cells

When [ $^3\text{H}$ ]-MitoQ was added to cells it was rapidly taken up and converted to the ubiquinol form within 10 min and then remained stable at 50–60% reduced (Figure 7A), similar to the redox state in isolated mitochondria. The redox state of [ $^3\text{H}$ ]-MitoQ in the extracellular medium also became reduced over time, equilibrating with the redox state of intracellular MitoQ within 2 h (Figure 7A), presumably by molecular exchange.

To see whether MitoQ reduction within cells was set by cell metabolism, we added the reduced form, [ $^3\text{H}$ ]-MitoQH<sub>2</sub>. [ $^3\text{H}$ ]-MitoQH<sub>2</sub> was rapidly oxidized and within 20 min reached a stable steady state level of 40–60% reduction, the same as that following addition of oxidized MitoQ (data not shown). The redox state of [ $^3\text{H}$ ]-MitoQ was also unaffected when the amount of added MitoQ was varied from 125 nM to 1  $\mu\text{M}$ , or when the [O<sub>2</sub>] was decreased from 21% to 3% (data not shown). The reduction of exogenous MitoQ was not cell type-specific, as [ $^3\text{H}$ ]-MitoQ added to C2C12 cells rapidly reached a steady state level of reduction similar to that of Jurkat cells (data not shown). When cells were incubated with [ $^3\text{H}$ ]-MitoQ in the presence of rotenone, the [ $^3\text{H}$ ]-MitoQ became less reduced (30  $\pm$  4%) while addition of the complex III inhibitor antimycin caused the [ $^3\text{H}$ ]-MitoQ to become more reduced (87  $\pm$  7%) (Figure 7B). Together these data indicate that the redox state of MitoQ within cells responds to that of the mitochondrial CoQ pool, and that reduction of MitoQ occurs rapidly, consistent with its fast uptake into mitochondria within cells.

To see how stable MitoQ was within cells, we incubated Jurkat cells with [ $^3\text{H}$ ]-MitoQ for 1, 24 and 48 h, and assayed for metabolites of [ $^3\text{H}$ ]-MitoQ by separating cell extracts by RP-HPLC and measuring the radioactivity in all fractions (Figure 7C). Over 48 h [ $^3\text{H}$ ]-MitoQ remained predominantly (~60–80%) in the reduced form (data not shown). After 1 h 99% of the radioactivity co-eluted with [ $^3\text{H}$ ]-MitoQH<sub>2</sub> or [ $^3\text{H}$ ]-MitoQ (Figure 7C), with no detectable MitoQ metabolites. At 24 and 48 h one new peak that accounted for 1–2% of the  $^3\text{H}$  radioactivity at 24 h and 12  $\pm$  6% at 48 h appeared on the HPLC trace. To identify the metabolite, equivalent fractions from parallel 48 h incubations with unlabelled MitoQ were isolated by HPLC and analyzed by ESI-MS. The metabolite peak contained a species of  $m/z$  = 665.3 that by tandem mass spectrometry readily fragmented to MitoQH<sub>2</sub> ( $m/z$  = 585.4) with a loss of 79.9 Da. The MitoQ mass was further fragmented to give a daughter ion of 262 Da, diagnostic of the TPP moiety confirming that the metabolite was a derivative of MitoQ. These data are consistent with the metabolite being sulfated MitoQ ( $m/z$  = 665.2 Da) which on loss of a sulfate (80.05 Da) regenerates MitoQuinol (Figure 1). This is in agreement with animal and cell data where monosulfated MitoQ was a major metabolite [43, 44]. Therefore, within cells MitoQ is rapidly reduced and attains a stable steady state level of the ubiquinol over long term incubations. Over 48 h some MitoQ is metabolised to a sulfated derivative, but the majority remains in the active ubiquinol form.

### DISCUSSION

The targeting of probes and bioactive molecules to mitochondria by conjugation to lipophilic cations such as TPP plays an increasing role in reporting on and modifying mitochondrial function. These molecules generally comprise relatively bulky and hydrophobic groups attached to a TPP moiety that drives their selective uptake into mitochondria. However, it

was unknown how these hydrophobic additions to the TPP molecule affected the rate and extent of their uptake into mitochondria within cells. Here, by comparing the uptake of MitoQ and DecylTPP into mitochondria and cells with the hydrophilic TPP cation TPMP, we have shown how the hydrophobicity of TPP cations affects their uptake.

The uptake of MitoQ into mitochondria and cells was described by the Nernst equation. Previous preliminary studies suggested that saturation of binding might lead to deviations from Nernstian behavior [13]. However, comparing the uptake of MitoQ with that of  $^{86}\text{Rb}^+$  showed that MitoQ uptake into mitochondria is fully described by the Nernst equation and that MitoQ bound extensively (>90%) within the mitochondrial matrix. Due to this binding, the total amount in mitochondria is about 10-fold greater than simple equilibration of the free compound with the  $\Delta\psi_m$ , and was ~5-fold greater than that of TPMP. This binding is most likely to be to the matrix facing surface of the inner membrane, with the TPP compounds adsorbed as a monolayer on the membrane with the TPP cation in a potential energy well close to the surface with the hydrophobic side chain inserted into the membrane [14, 21]. Such a location for hydrophobic TPP derivatives is fortuitous as many mitochondrial activities are associated with the inner membrane.

The extent of uptake of MitoQ into mitochondria within cells was also 4–5-fold greater than that of TPMP and was also consistent with the Nernst equation. In the cytosol most MitoQ was bound. The uptake was selective for mitochondria with the majority of MitoQ in the cell being concentrated within mitochondria due to the  $\Delta\psi_m$ .

Increasing the hydrophobicity of TPP molecules increased their rate of uptake into cells several-fold. This increase was due to the far more rapid permeation of the plasma membrane by the hydrophobic TPP compounds. The reason for this is likely to be the greater hydrophobicity of MitoQ and DecylTPP lowering their activation energies for plasma membrane passage (octan-1-ol:PBS partition coefficients: MitoQ ~3000, DecylTPP ~5000, TPMP = 0.35) [26]. The activation energy for transport of lipophilic cations through a phospholipid bilayer is made up of an unfavorable Born energy due to the charge of the TPP moiety that is the same for all TPP cations and a favorable hydrophobic force that is the main difference between molecules such as MitoQ and TPMP [14]. That the plasma membrane acts as a significant kinetic barrier to movement of hydrophilic TPP cations is strongly supported by the fact that the lipophilic tetraphenylborate anion (TPB) is routinely added to speed up equilibration of TPMP into cells and does so by lowering the activation energy for membrane transport [14, 39, 45]. TPB is not required to assist the uptake of TPMP through the mitochondrial inner membrane suggesting that the activation energy for transport across this membrane is lower. Lipophilic dications are also more readily taken up through the mitochondrial inner membrane than the plasma membrane and increasing their hydrophobicity increases their uptake through the plasma membrane [31]. Several factors may contribute to this difference in activation energies between the mitochondrial and plasma membranes, including their different phospholipid compositions, lack of cholesterol and presence of cardiolipin in the inner membrane, the difference in  $\Delta\psi$  values and the very high protein content of the inner membrane which may increase its dielectric constant [42].

Once past the plasma membrane MitoQ and DecylTPP were taken up rapidly into mitochondria, as evidenced by the predominantly mitochondrial localisation of the MitoQ analogue IDTP and by the fact that the uptake of MitoQ and DecylTPP into cells was greatly decreased by FCCP. MitoQ was rapidly reduced to its ubiquinol form by the mitochondrial respiratory chain, further supporting mitochondrial localization within cells. As this reduction had the same kinetic profiles as uptake into cells, it is concluded that these compounds are rapidly accumulated by mitochondria once within cells.

In cells MitoQ rapidly becomes 50-60% reduced to the ubiquinol form. MitoQ is stably retained in the reduced form within cells over at least 48 h. Over this time there was some metabolism to a sulfated derivative, but most of the added MitoQ persisted and was predominantly reduced. These findings are consistent with the protective effects seen with MitoQ in cell and animal models being due to MitoQH<sub>2</sub> preventing lipid peroxidation within mitochondria [41].

To summarise, uptake of lipophilic TPP cations into mitochondria is described by the Nernst equation, is rapid compared to its metabolism and it equilibrates rapidly with the CoQ pool. A model for the uptake of MitoQ by cells that is consistent with our findings is illustrated in Figure 8. The Nernst equation relates free, unbound pools of compound that equilibrate with the  $\Delta\psi_p$  and  $\Delta\psi_m$ . Extracellular MitoQ is ~ 78% bound to serum, and the free MitoQ then equilibrates with the free concentration within the cytosol in response to the  $\Delta\psi_p$ . This free concentration is then in equilibrium with the >99% of cytosolic MitoQ that is bound. The free MitoQ in the cytosol is in turn in equilibrium with the free concentration within the mitochondrial matrix, and this relationship is determined by the  $\Delta\psi_m$ . The free pool of MitoQ in the matrix is in equilibrium with a 10-fold excess that is bound to the matrix face of the mitochondrial inner membrane. These findings suggest that mitochondria-targeted compounds can be optimised by adjusting their hydrophobicity to modulate their rates of uptake into cells, and the extent of their uptake and concentration in the matrix by altering their binding to the mitochondrial inner membrane. Through such modifications it should be possible to design rationally further compounds to manipulate and report on particular mitochondrial functions.

This work was supported by the Medical Research Council (UK), Antipodean Pharmaceuticals Inc. and by the European Community's 6<sup>th</sup> Framework Programme for Research, Priority 1 "Life sciences, genomics and biotechnology for health" Contract LSHM-CT-2004-503116. We thank Dr. Abdul-Rahman bin Manas and Pauline Bandeen for technical assistance with the synthetic chemistry, Stephanie Brown for technical assistance and Martin Brand for helpful discussions on the manuscript.

## REFERENCES

- 1 Murphy, M. P. and Smith, R. A. (2007) Targeting antioxidants to mitochondria by conjugation to lipophilic cations. *Annu. Rev. Pharmacol. Toxicol.* **47**, 629-656
- 2 Burns, R. J., Smith, R. A. J. and Murphy, M. P. (1995) Synthesis and characterization of thiobutyltriphenylphosphonium bromide, a novel thiol reagent targeted to the mitochondrial matrix. *Arch. Biochem. Biophys.* **322**, 60-68
- 3 Smith, R. A. J., Porteous, C. M., Coulter, C. V. and Murphy, M. P. (1999) Targeting an antioxidant to mitochondria. *Eur. J. Biochem.* **263**, 709-716
- 4 Hardy, M., Chalier, F., Ouari, O., Finet, J. P., Rockenbauer, A., Kalyanaraman, B. and Tordo, P. (2007) Mito-DEPMPO synthesized from a novel NH<sub>2</sub>-reactive DEPMPO spin trap: a new and improved trap for the detection of superoxide. *Chem. Commun.* **10**, 1083-1085
- 5 Xu, Y. and Kalyanaraman, B. (2007) Synthesis and ESR studies of a novel cyclic nitron spin trap attached to a phosphonium group—a suitable trap for mitochondria-generated ROS? *Free Radic. Res.* **41**, 1-7
- 6 Robinson, K. M., Janes, M. S., Pehar, M., Monette, J. S., Ross, M. F., Hagen, T. M., Murphy, M. P. and Beckman, J. S. (2006) Selective fluorescent imaging of

- superoxide in vivo using ethidium-based probes. *Proc. Natl. Acad. Sci. USA.* **103**, 15038-15043
- 7 James, A. M., Blaikie, F. H., Smith, R. A., Lightowers, R. N., Smith, P. M. and Murphy, M. P. (2003) Specific targeting of a DNA-alkylating reagent to mitochondria. Synthesis and characterization of [4-((11aS)-7-methoxy-1,2,3,11a-tetrahydro-5H-pyrrolo[2,1-c][1,4]benzodiazepin-5-on-8-oxy)butyl]-triphenylphosphonium iodide. *Eur. J. Biochem.* **270**, 2827-2836
- 8 Filipovska, A., Kelso, G. F., Brown, S. E., Beer, S. M., Smith, R. A. and Murphy, M. P. (2005) Synthesis and characterization of a triphenylphosphonium-conjugated peroxidase mimetic: Insights into the interaction of ebselen with mitochondria. *J. Biol. Chem.* **280**, 24113-24126
- 9 Dhanasekaran, A., Kotamraju, S., Karunakaran, C., Kalivendi, S. V., Thomas, S., Joseph, J. and Kalyanaraman, B. (2005) Mitochondria superoxide dismutase mimetic inhibits peroxide-induced oxidative damage and apoptosis: role of mitochondrial superoxide. *Free Radic. Biol. Med.* **39**, 567-583
- 10 Muratovska, A., Lightowers, R. N., Taylor, R. W., Turnbull, D. M., Smith, R. A. J., Wilce, J. A., Martin, S. W. and Murphy, M. P. (2001) Targeting peptide nucleic acid (PNA) oligomers to mitochondria within cells by conjugation to lipophilic cations: implications for mitochondrial DNA replication, expression and disease. *Nucleic Acids Res.* **29**, 1852-1863
- 11 Lin, T. K., Hughes, G., Muratovska, A., Blaikie, F. H., Brookes, P. S., Darley-Usmar, V., Smith, R. A. J. and Murphy, M. P. (2002) Specific modification of mitochondrial protein thiols in response to oxidative stress: a proteomics approach. *J. Biol. Chem.* **277**, 17048-17056
- 12 Murphy, M. P., Echtay, K. S., Blaikie, F. H., Asin-Cayuela, J., Cochemé, H. M., Green, K., Buckingham, J. A., Taylor, E. R., Hurrell, F., Hughes, G., Miwa, S., Cooper, C. E., Svistunenko, D. A., Smith, R. A. and Brand, M. D. (2003) Superoxide activates uncoupling proteins by generating carbon-centered radicals and initiating lipid peroxidation: studies using a mitochondria-targeted spin trap derived from alpha-phenyl-N-tert-butyl nitron. *J. Biol. Chem.* **278**, 48534-48545
- 13 Kelso, G. F., Porteous, C. M., Coulter, C. V., Hughes, G., Porteous, W. K., Ledgerwood, E. C., Smith, R. A. J. and Murphy, M. P. (2001) Selective targeting of a redox-active ubiquinone to mitochondria within cells. *J. Biol. Chem.* **276**, 4588 - 4596
- 14 Ross, M. F., Kelso, G. F., Blaikie, F. H., James, A. M., Cochemé, H. M., Filipovska, A., Da Ros, T., Hurd, T. R., Smith, R. A. and Murphy, M. P. (2005) Lipophilic triphenylphosphonium cations as tools in mitochondrial bioenergetics and free radical biology. *Biochemistry (Mosc).* **70**, 222-230
- 15 Balaban, R. S., Nemoto, S. and Finkel, T. (2005) Mitochondria, oxidants, and aging. *Cell.* **120**, 483-495
- 16 Finkel, T. (2005) Opinion: Radical medicine: treating ageing to cure disease. *Nat. Rev. Mol. Cell. Biol.* **6**, 971-976
- 17 Jauslin, M. L., Meier, T., Smith, R. A. J. and Murphy, M. P. (2003) Mitochondria-targeted antioxidants protect Friedreich Ataxia fibroblasts from endogenous oxidative stress more effectively than untargeted antioxidants. *FASEB J.* **17**, 1972-1974

- 18 Adlam, V. J., Harrison, J. C., Porteous, C. M., James, A. M., Smith, R. A., Murphy, M. P. and Sammut, I. A. (2005) Targeting an antioxidant to mitochondria decreases cardiac ischemia-reperfusion injury. *FASEB J.* **19**, 1088-1095
- 19 Smith, R. A. J., Porteous, C. M., Gane, A. M. and Murphy, M. P. (2003) Delivery of bioactive molecules to mitochondria in vivo. *Proc. Natl. Acad. Sci. USA.* **100**, 5407-5412
- 20 James, A. M., Cochemé, H. M., Smith, R. A. and Murphy, M. P. (2005) Interactions of mitochondria-targeted and untargeted ubiquinones with the mitochondrial respiratory chain and reactive oxygen species. Implications for the use of exogenous ubiquinones as therapies and experimental tools. *J. Biol. Chem.* **280**, 21295-21312
- 21 James, A. M., Sharpley, M. S., Manas, A. R., Frerman, F. E., Hirst, J., Smith, R. A. and Murphy, M. P. (2007) Interaction of the mitochondria-targeted antioxidant MitoQ with phospholipid bilayers and ubiquinone oxidoreductases. *J. Biol. Chem.* **282**, 14708-14718
- 22 Kalivendi, S. V., Konorev, E. A., Cunningham, S., Vanamala, S. K., Kaji, E. H., Joseph, J. and Kalyanaraman, B. (2005) Doxorubicin activates nuclear factor of activated T-lymphocytes and Fas ligand transcription: role of mitochondrial reactive oxygen species and calcium. *Biochem. J.* **389**, 527-539
- 23 Esplugues, J. V., Rocha, M., Nunez, C., Bosca, I., Ibiza, S., Herance, J. R., Ortega, A., Serrador, J. M., D'Ocon, P. and Victor, V. M. (2006) Complex I dysfunction and tolerance to nitroglycerin: an approach based on mitochondrial-targeted antioxidants. *Circ. Res.* **99**, 1067-1075
- 24 Neuzil, J., Widen, C., Gellert, N., Swettenham, E., Zabalova, R., Dong, L. F., Wang, X. F., Lidebjer, C., Dalen, H., Headrick, J. P. and Witting, P. K. (2007) Mitochondria transmit apoptosis signalling in cardiomyocyte-like cells and isolated hearts exposed to experimental ischemia-reperfusion injury. *Redox Rep.* **12**, 148-162
- 25 [www.antipodeanpharma.com](http://www.antipodeanpharma.com).
- 26 Asin-Cayuela, J., Manas, A. R., James, A. M., Smith, R. A. and Murphy, M. P. (2004) Fine-tuning the hydrophobicity of a mitochondria-targeted antioxidant. *FEBS Lett.* **571**, 9-16
- 27 Taylor, K. M. and Smith, R. A. J. (2006) Preparation of mitoquinone derivatives as mitochondrially targeted antioxidants. US Patent Application 2006-355518
- 28 Smith, R. A., Kelso, G. F., James, A. M. and Murphy, M. P. (2004) Targeting coenzyme Q derivatives to mitochondria. *Methods Enzymol.* **382**, 45-67
- 29 Chappell, J. B. and Hansford, R. G. (1972) Preparation of mitochondria from animal tissues and yeasts. In *Subcellular components: preparation and fractionation* (Birnie, G. D., ed.). pp. 77-91, Butterworths, London
- 30 Gornall, A. G., Bardawill, C. J. and David, M. M. (1949) Determination of serum protein by means of the biuret reaction. *J. Biol. Chem.* **177**, 751-766
- 31 Ross, M. F., Da Ros, T., Blaikie, F. H., Prime, T. A., Porteous, C. M., Severina, I. I., Skulachev, V. P., Kjaergaard, H. G., Smith, R. A. and Murphy, M. P. (2006) Accumulation of lipophilic dicationic antioxidants by mitochondria and cells. *Biochem. J.* **400**, 199-208
- 32 Brand, M. D. (1995) Measurement of mitochondrial protonmotive force. In *Bioenergetics - a practical approach* (Brown, G. C. and Cooper, C. E., eds.). pp. 39-62, IRL, Oxford

- 33 Brown, S. E., Ross, M. F., Sanjuan-Pla, A., Manas, A. R., Smith, R. A. and Murphy, M. P. (2007) Targeting lipoic acid to mitochondria: synthesis and characterization of a triphenylphosphonium-conjugated alpha-lipoyl derivative. *Free Radic. Biol. Med.* **42**, 1766-1780
- 34 Scarlett, J. L., Sheard, P. W., Hughes, G., Ledgerwood, E. C., Ku, H.-H. and Murphy, M. P. (2000) Changes in mitochondrial membrane potential during staurosporine-induced apoptosis in Jurkat cells. *FEBS Letts.* **475**, 267-272
- 35 Nobes, C. D., Brown, G. C., Olive, P. N. and Brand, M. D. (1990) Non-ohmic proton conductance of the mitochondrial inner membrane in hepatocytes. *J. Biol. Chem.* **265**, 12903-12909
- 36 Ross, M. F., Filipovska, A., Smith, R. A., Gait, M. J. and Murphy, M. P. (2004) Cell-penetrating peptides do not cross mitochondrial membranes even when conjugated to a lipophilic cation: evidence against direct passage through phospholipid bilayers. *Biochem. J.* **383**, 457-468
- 37 Brown, G. C. and Brand, M. D. (1985) Thermodynamic control of electron flux through mitochondrial cytochrome *bc<sub>1</sub>* complex. *Biochem. J.* **225**, 399-405
- 38 Scott, I. D. and Nicholls, D. G. (1980) Energy transduction in intact synaptosomes. *Biochem. J.* **186**, 21-33
- 39 Brand, M. D. and Felber, S. M. (1984) Membrane potential of mitochondria in intact lymphocytes during early mitogenic stimulation. *Biochem. J.* **217**, 453-459
- 40 Nicholls, D. G. (2006) Simultaneous monitoring of ionophore- and inhibitor-mediated plasma and mitochondrial membrane potential changes in cultured neurons. *J. Biol. Chem.* **281**, 14864-14874
- 41 Koopman, W. J., Verkaart, S., Visch, H. J., van der Westhuizen, F. H., Murphy, M. P., van den Heuvel, L. W., Smeitink, J. A. and Willems, P. H. (2005) Inhibition of complex I of the electron transport chain causes O<sub>2</sub><sup>-</sup>-mediated mitochondrial outgrowth. *Am. J. Physiol. Cell. Physiol.* **288**, C1440-1450
- 42 Murphy, M. P. (1989) Slip and leak in mitochondrial oxidative phosphorylation. *Biochim. Biophys. Acta.* **977**, 123-141
- 43 Li, Y., Zhang, H., Fawcett, J. P. and Tucker, I. G. (2007) Quantitation and metabolism of mitoquinone, a mitochondria-targeted antioxidant, in rat by liquid chromatography/tandem mass spectrometry. *Rapid Commun. Mass Spectrom.* **21**, 1958-1964
- 44 Li, Y., Fawcett, J. P., Zhang, H. and Tucker, I. G. (2007) Transport and metabolism of MitoQ<sub>10</sub>, a mitochondria-targeted antioxidant, in Caco-2 cell monolayers. *J. Pharm. Pharmacol.* **59**, 503-511
- 45 James, A. M., Wei, Y.-H., Pang, C.-Y. and Murphy, M. P. (1996) Altered mitochondrial function in fibroblasts containing MELAS or MERRF mitochondrial DNA mutations. *Biochem. J.* **318**, 401-407

### Figure legends

#### Figure 1 Structures of MitoQ, MitoQH<sub>2</sub>, DecylTPP, TPMP, IDTP and a sulfated metabolite of MitoQ

While MitoQ is sulfated on only one phenolic oxygen it is not known which.

#### Figure 2 Uptake of [<sup>3</sup>H]-MitoQ and [<sup>3</sup>H]-TPMP by mitochondria over a range of $\Delta\psi_m$ values

(A) The TPMP accumulation ratio (ACR) within isolated mitochondria is a linear function of the <sup>86</sup>Rb<sup>+</sup> accumulation ratio: TPMP ACR = 2.1 x Rb<sup>+</sup> ACR. (B) The MitoQ accumulation ratio within isolated mitochondria is also a linear function of the Rb<sup>+</sup> accumulation ratio: MitoQ ACR = 10.3 x Rb ACR + 8600. (C) Quantitation of MitoQ binding to mitochondria in the absence of  $\Delta\psi_m$ . MitoQ bound to mitochondria in the absence of  $\Delta\psi_m$  is proportional to the concentration of MitoQ free in solution, and is described by the relationship: MitoQ(bound; pmol.mg protein<sup>-1</sup>) = 5.1 x MitoQ (free; nM). The bound/free ratio for 1  $\mu$ M TPMP (0.038 (pmol.mg protein<sup>-1</sup>).nM<sup>-1</sup>) is also shown. (D) Relationship between MitoQ ACR and Rb<sup>+</sup> ACR when  $\Delta\psi_m$ -independent binding is accounted for. The concentration of free MitoQ (i.e. MitoQ in the supernatant after isolation of mitochondria) in the samples shown in (B) was used to quantitate  $\Delta\psi_m$ -independent binding of MitoQ using the equation from Figure 2C. This was subtracted from the total amount of mitochondria-associated MitoQ in the samples shown in (B), and a new ACR calculated. The data for the TPMP accumulation ratio from Figure 2A are included for comparison. (A-D) show representative data from single experiments that were repeated at least three times. Lines of best fit were determined with Excel software. (E) Variation of mitochondrial uptake of TPMP and MitoQ with  $\Delta\psi_m$  at a fixed extramitochondrial concentration of 10 nM. (F) Variation of mitochondrial uptake of TPMP and MitoQ with extramitochondrial concentration at a fixed  $\Delta\psi_m$  of 150 mV. For (E) and (F) mitochondrial uptake was modelled using the equations generated in (D).

#### Figure 3 [<sup>3</sup>H]-MitoQ and [<sup>3</sup>H]-DecylTPP uptake into cells is rapid, extensive and FCCP-sensitive

(A) MitoQ and TPMP uptake by cells over 23 h. Jurkat cells (3 x 10<sup>6</sup>.mL<sup>-1</sup>) were incubated with 500 nM [<sup>3</sup>H]-MitoQ or [<sup>3</sup>H]-TPMP for up to 23 h. Data are means of duplicate samples from a representative experiment that was repeated three times. (B) Uptake of [<sup>3</sup>H]-MitoQ, [<sup>3</sup>H]-DecylTPP and [<sup>3</sup>H]-TPMP into cells over 40 min. The conditions were as for (A). (C) Rates of MitoQ and TPMP efflux from Jurkat cells. Cells were incubated with [<sup>3</sup>H]-MitoQ or [<sup>3</sup>H]-TPMP as above for 3 and 6 h, respectively, then 5  $\mu$ M FCCP was added and the amounts of [<sup>3</sup>H]-MitoQ or [<sup>3</sup>H]-TPMP left in the cells were measured at the indicated times. The inset shows a plot of the natural log of the efflux data for the two compounds. The slopes of these lines gave the first order rate constants and half-lives for the FCCP-induced efflux of MitoQ and TPMP from Jurkat cells. (D) MitoQ, DecylTPP and TPMP uptake by cells  $\pm$  FCCP. Jurkat cells were incubated for 3 h with 500  $\mu$ M [<sup>3</sup>H]-MitoQ, [<sup>3</sup>H]-TPMP, or for 9 h with [<sup>3</sup>H]-TPMP  $\pm$  5  $\mu$ M FCCP. Data are means  $\pm$  SD from at least three independent experiments, each determined in duplicate.

#### Figure 4 IDTP localises predominantly to mitochondria within cultured human fibroblasts

Cells were incubated with 1  $\mu\text{M}$  IDTP for 3.5 h  $\pm$  5  $\mu\text{M}$  FCCP. MitoTracker Orange was added for the last 30 min. The cells were then fixed and treated with antiserum against the TPP moiety of IDTP and a secondary antibody linked to Oregon Green 488. Scale bar = 20  $\mu\text{m}$ .

#### Figure 5 [ $^3\text{H}$ ]-MitoQ and [ $^3\text{H}$ ]-TPMP uptake into cells driven by the $\Delta\psi_p$

(A) MitoQ uptake into cells driven by  $\Delta\psi_p$  over 40 min. Jurkat cells ( $3 \times 10^6 \cdot \text{mL}^{-1}$ ) were incubated with 500 nM [ $^3\text{H}$ ]-MitoQ for up to 40 min in the presence or absence of the mitochondrial inhibitors oligomycin and myxothiazol. Data are means of duplicate samples from a representative experiment that was repeated once. (B) Stability of  $\Delta\psi_p$  in the presence of oligomycin and myxothiazol. PMPI was used to follow changes in Jurkat cell  $\Delta\psi_p$ . Additions of oligomycin and myxothiazol (both 5  $\mu\text{M}$ ) were made which showed no effect on  $\Delta\psi_p$ . Gramicidin (5  $\mu\text{g} \cdot \text{mL}^{-1}$ ) was added after 45 min to abolish the  $\Delta\psi_p$ . The approximate values of the resting  $\Delta\psi_p$  and of  $\Delta\psi_p$  in the presence of gramicidin are shown. Traces of the PMPI fluorescence of cells without addition of oligomycin and myxothiazol were similar to the trace shown. (C) Uptake of MitoQ into cells lacking a  $\Delta\psi_m$  (oligomycin/myxothiazol-treated). Quantification of MitoQ uptake after 40 min, in the presence of oligomycin/myxothiazol  $\pm$  gramicidin. Data are means  $\pm$  SD of three experiments each determined in duplicate; \* $p < 0.05$  Student's two-tailed  $t$  test. (D) Uptake of TPMP into cells lacking a  $\Delta\psi_m$ . Jurkat cells ( $3 \times 10^6 \cdot \text{mL}^{-1}$ ) were incubated with 500 nM [ $^3\text{H}$ ]-TPMP for up to 150 min in the presence or absence of the mitochondrial inhibitors oligomycin and myxothiazol  $\pm$  gramicidin. Data are means of duplicate samples from a representative experiment.

#### Figure 6 Redox state of MitoQ on incubation with mitochondria

(A) Detection and quantitation of [ $^3\text{H}$ ]-MitoQuinone ([ $^3\text{H}$ ]-MitoQ) and [ $^3\text{H}$ ]-MitoQuinol ([ $^3\text{H}$ ]-MitoQH<sub>2</sub>) following extraction from a mitochondrial incubation, separation by RP-HPLC and scintillation counting of collected fractions. (B) Redox poise of [ $^3\text{H}$ ]-MitoQ in energized mitochondria. Rat liver mitochondria respiring on succinate (10 mM) in the presence of rotenone (4  $\mu\text{g} \cdot \text{mL}^{-1}$ ) or glutamate and malate (5 mM of each) were incubated in the presence of 500 nM [ $^3\text{H}$ ]-MitoQ for 5 min. [ $^3\text{H}$ ]-MitoQuinone and [ $^3\text{H}$ ]-MitoQuinol were extracted and their ratio determined as described in (A). The effects of the uncoupler FCCP (0.5  $\mu\text{M}$ ) or of the inhibitors malonate (20 mM) and rotenone (4  $\mu\text{g} \cdot \text{mL}^{-1}$ ) are shown. (C) MitoQ redox poise in intact mitochondria, in the presence of the uncoupler FCCP. [ $^3\text{H}$ ]-MitoQ was incubated with mitochondria as in (B) for 5 min in the presence of FCCP along with rotenone and succinate, or glutamate/malate, for 5 min and then the [ $^3\text{H}$ ]-MitoQuinone and [ $^3\text{H}$ ]-MitoQuinol were extracted and their ratio determined as described in (A). The effect of preincubation with the inhibitors myxothiazol (2  $\mu\text{M}$ ), malonate (20 mM), and rotenone (4  $\mu\text{g} \cdot \text{mL}^{-1}$ ) on the redox poise of MitoQ were then determined. Data in (B & C) are means  $\pm$  SD  $n = 3-8$  \* $p < 0.05$  \*\* $p < 0.005$  \*\*\* $p < 0.0005$ ; n.s.  $p > 0.05$  by Student's two-tailed  $t$  test.

**Figure 7 Reduction and metabolism of [<sup>3</sup>H]-MitoQ by cells**

(A) Time course of MitoQ reduction by cells. Jurkat cells were incubated with 500 nM [<sup>3</sup>H]-MitoQ as described in Figure 3A and at the indicated times cells were pelleted and the percentage of [<sup>3</sup>H]-MitoQ in the cells (black squares) or supernatant (open squares) that was reduced was determined as described in Figure 6A. (B) The effect of respiratory inhibitors on the redox state of MitoQ in cells. [<sup>3</sup>H]-MitoQ was incubated with Jurkat cells as described in (A) and after 1 h the ratio of reduced to oxidized MitoQ in the cells was determined by extraction, RP-HPLC and scintillation counting as described in Figure 6A. The effect on this of the respiratory inhibitors rotenone (4  $\mu\text{g}\cdot\text{mL}^{-1}$ ) and antimycin A (1  $\mu\text{M}$ ) are shown. Data are means  $\pm$  SD of at least three independent experiments, each of which was done in duplicate. (C) Metabolism of MitoQ by cells. Jurkat cells were incubated with 500 nM [<sup>3</sup>H]-MitoQ for 1, 24 and 48 h. At these times [<sup>3</sup>H]-MitoQ and any metabolites were extracted and separated by RP-HPLC and all fractions counted for radioactivity. Over 24 and 48 h a radioactive metabolite of MitoQ was detected on the HPLC profile (arrow). (D) Quantitation of the MitoQ metabolite over time. The metabolite indicated by the arrowhead in (C) is expressed as a percentage of the total radioactivity recovered from the HPLC analysis shown in (C). Data at 48 h are means  $\pm$  SD of three determinations.

**Figure 8 Uptake and distribution of MitoQ and related compounds in cells**

The equilibrium distribution of free MitoQ within a cell with a  $\Delta\psi_p$  of 40 mV and a  $\Delta\psi_m$  of 150 mV was calculated from the Nernst equation. The indicated proportions of MitoQ bound were determined from the binding constants derived in the text. The values in square brackets are the approximate relative concentration free or bound in the different compartments. The total amounts of MitoQ present in each compartment will vary depending on the cell and mitochondrial volumes.

Figure 1

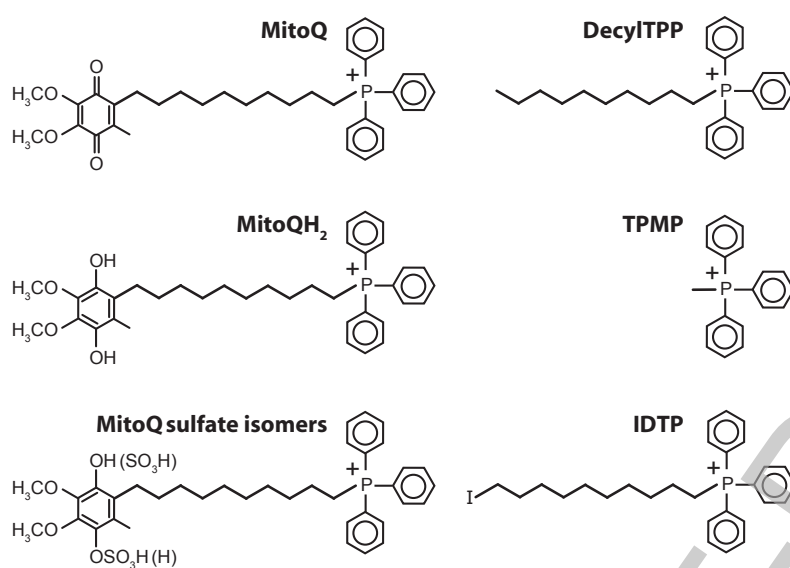
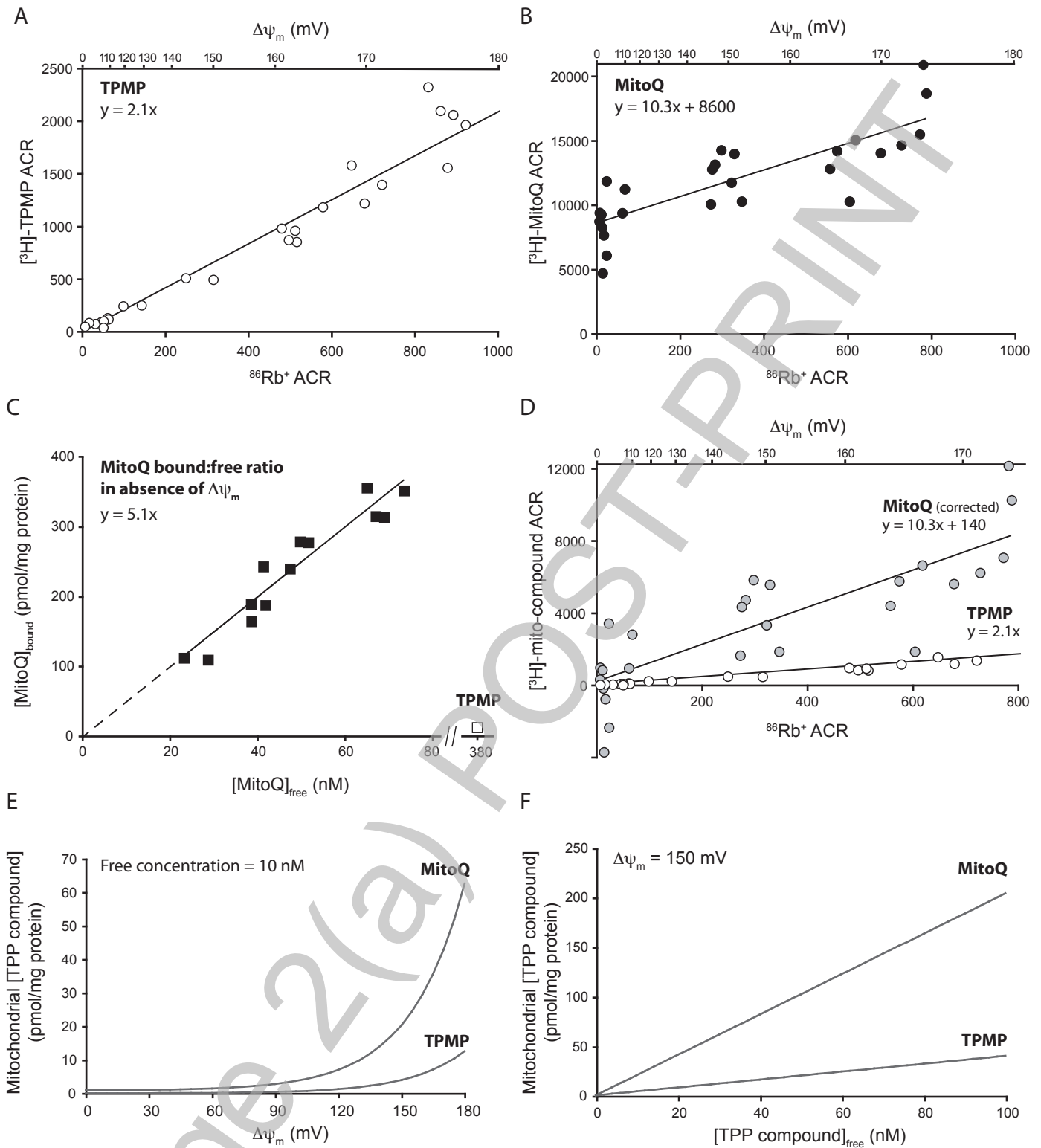


Figure 2



THIS IS NOT THE FINAL VERSION - see doi:10.1042/BJ20080063

Figure 3

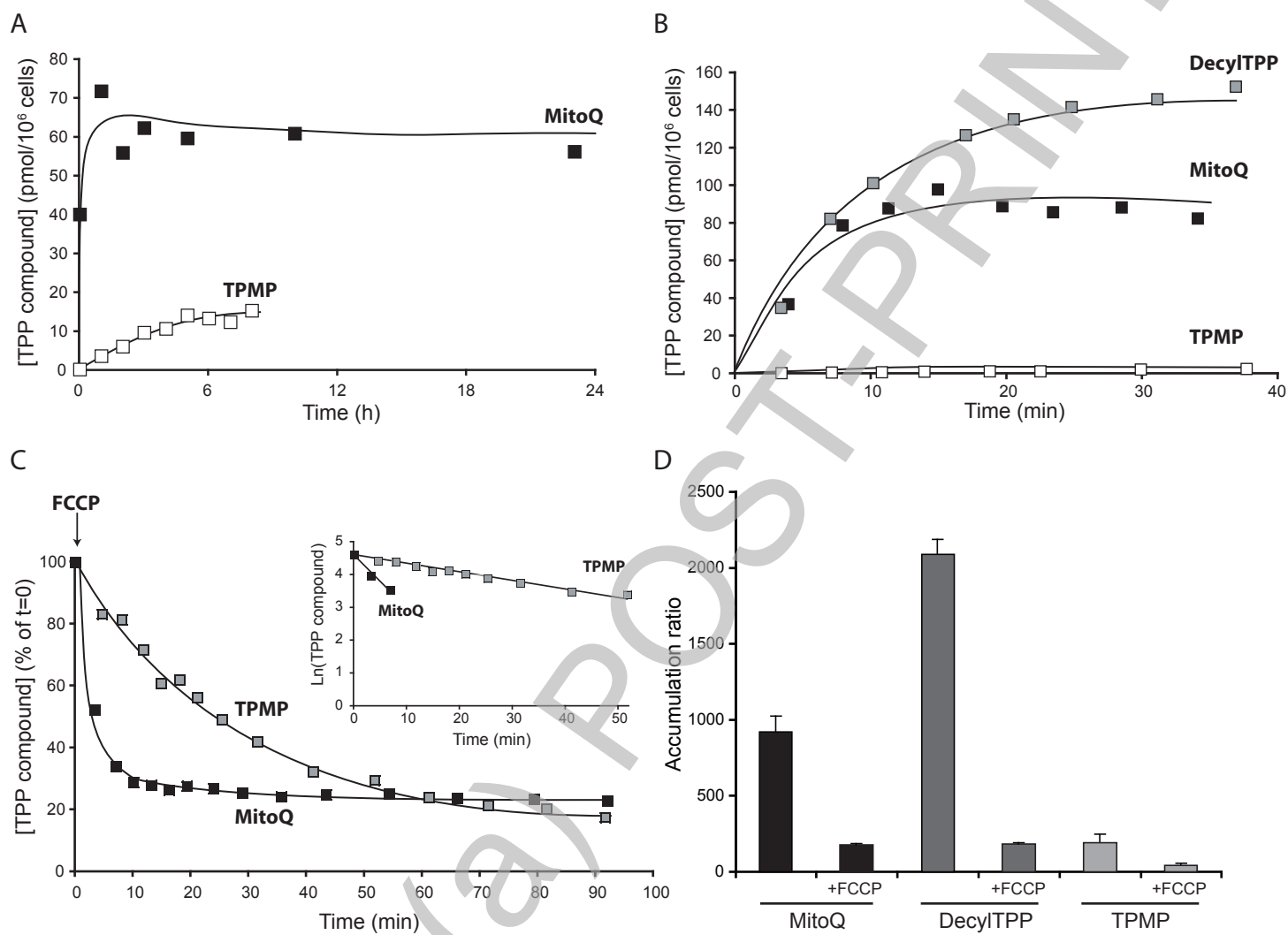
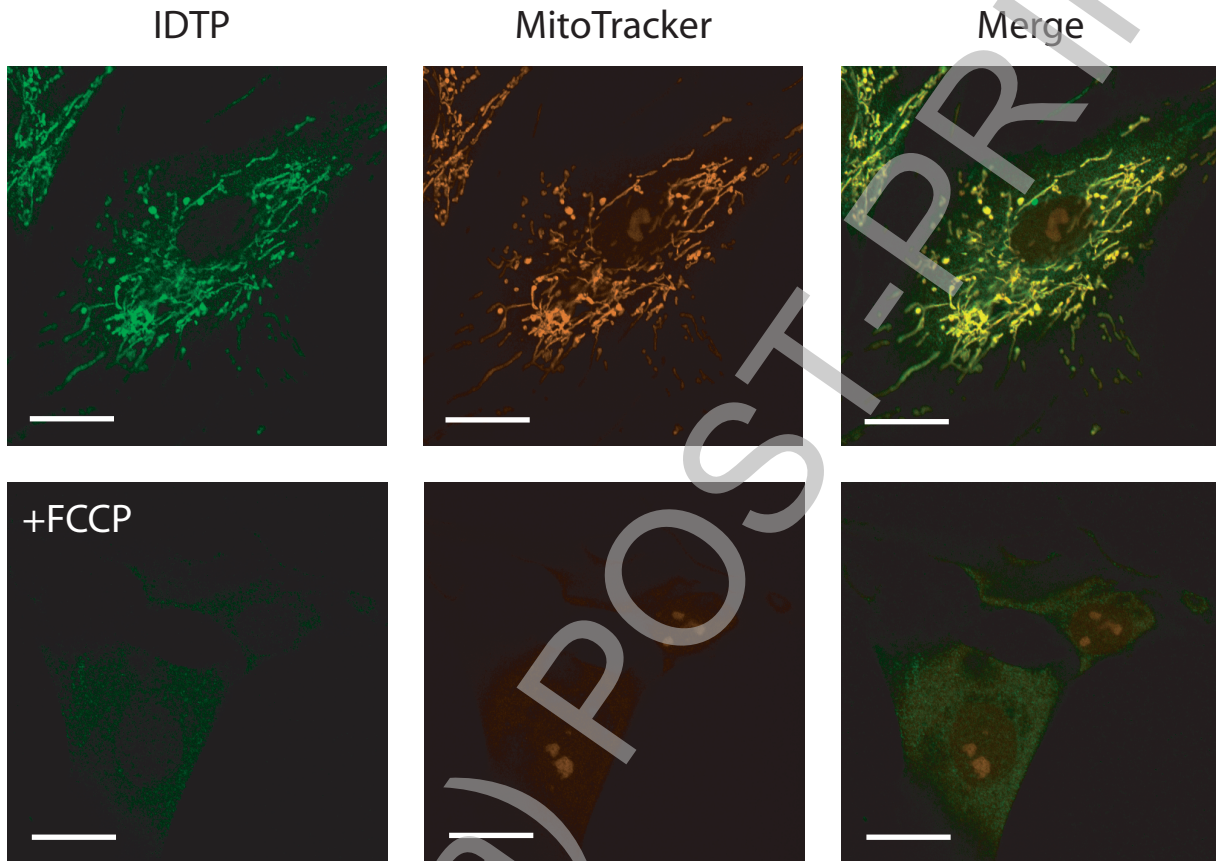


Figure 4



THIS IS NOT THE FINAL VERSION - see doi:10.1042/BJ20080063

Stage 2(a) POST-PRINT

Figure 5

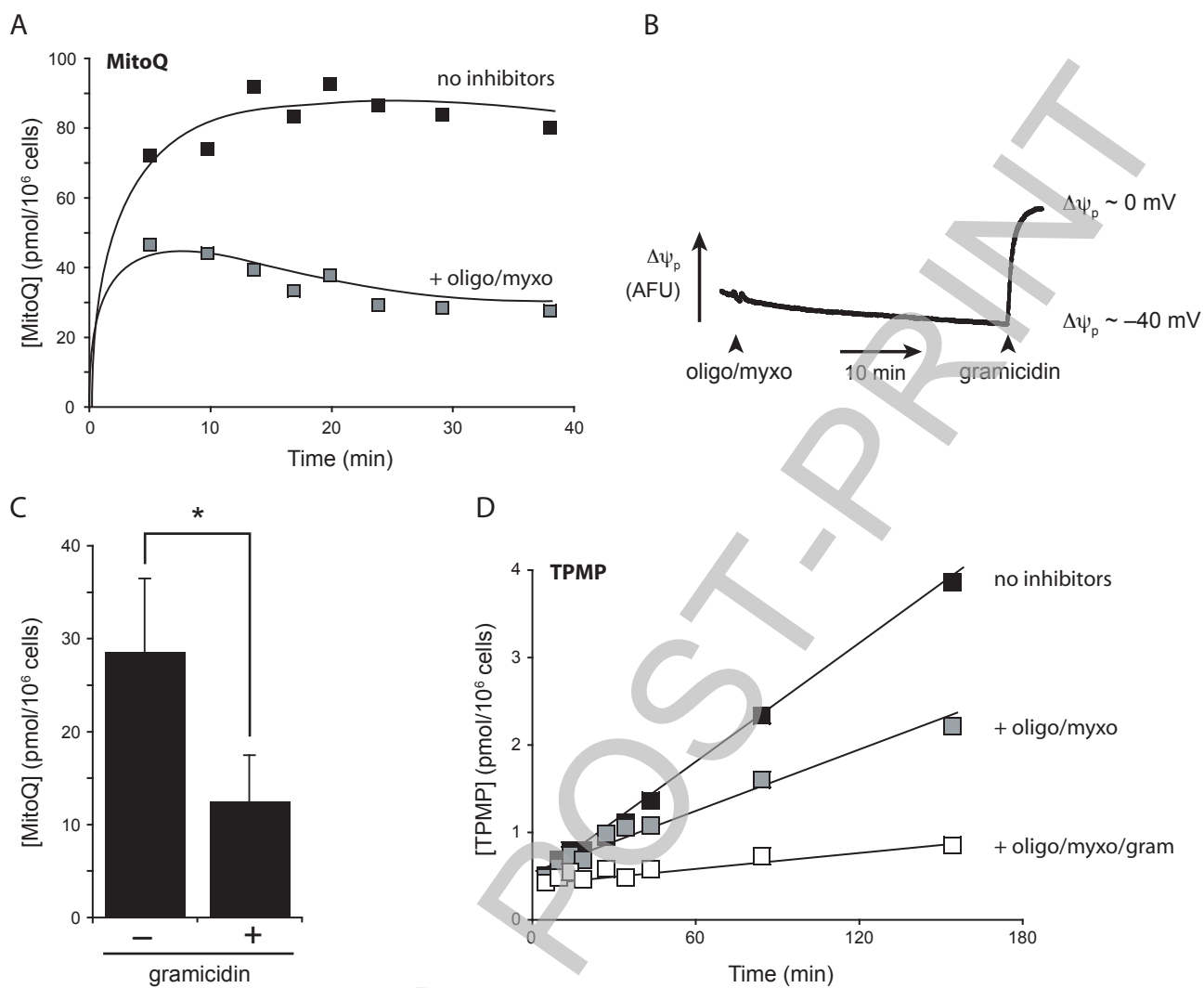
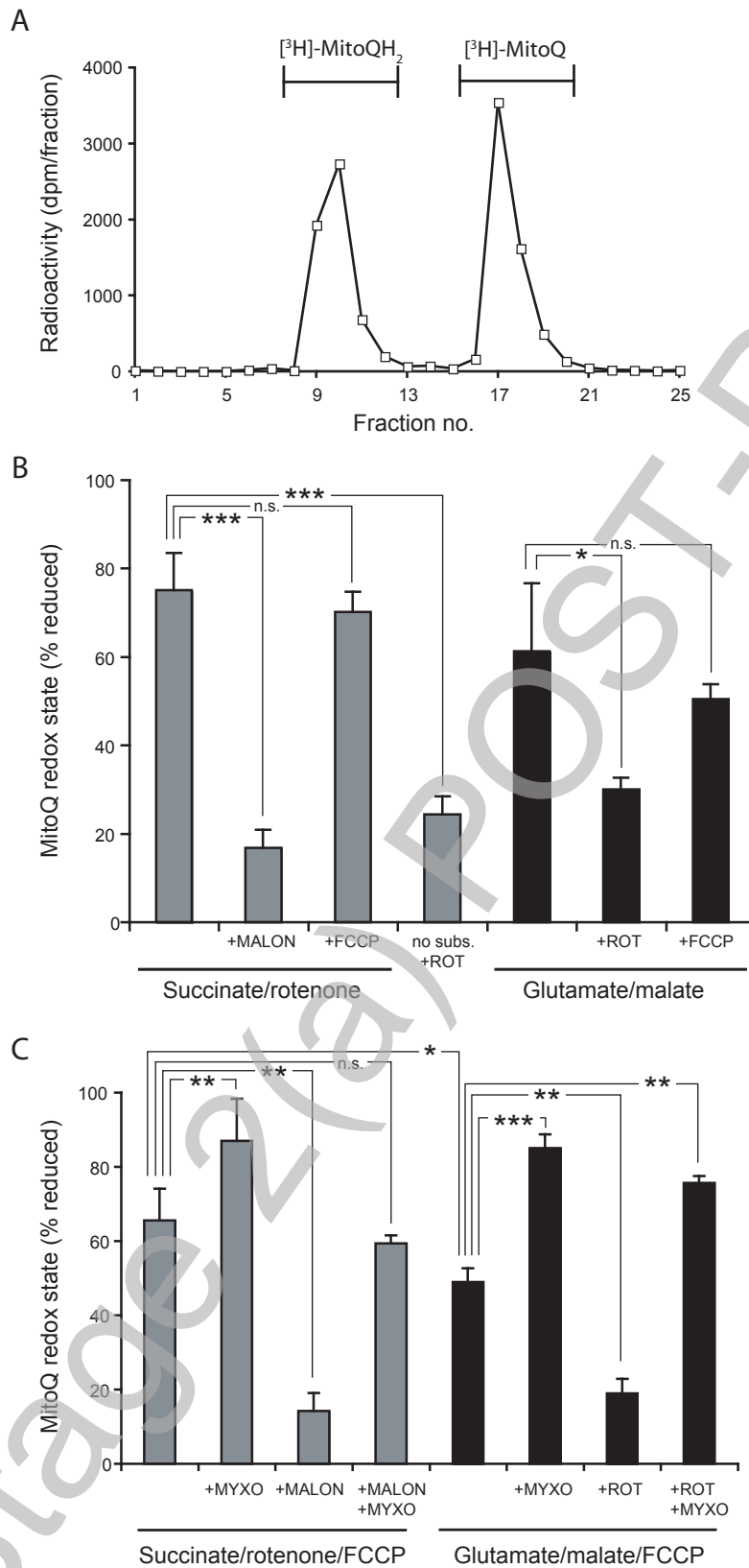
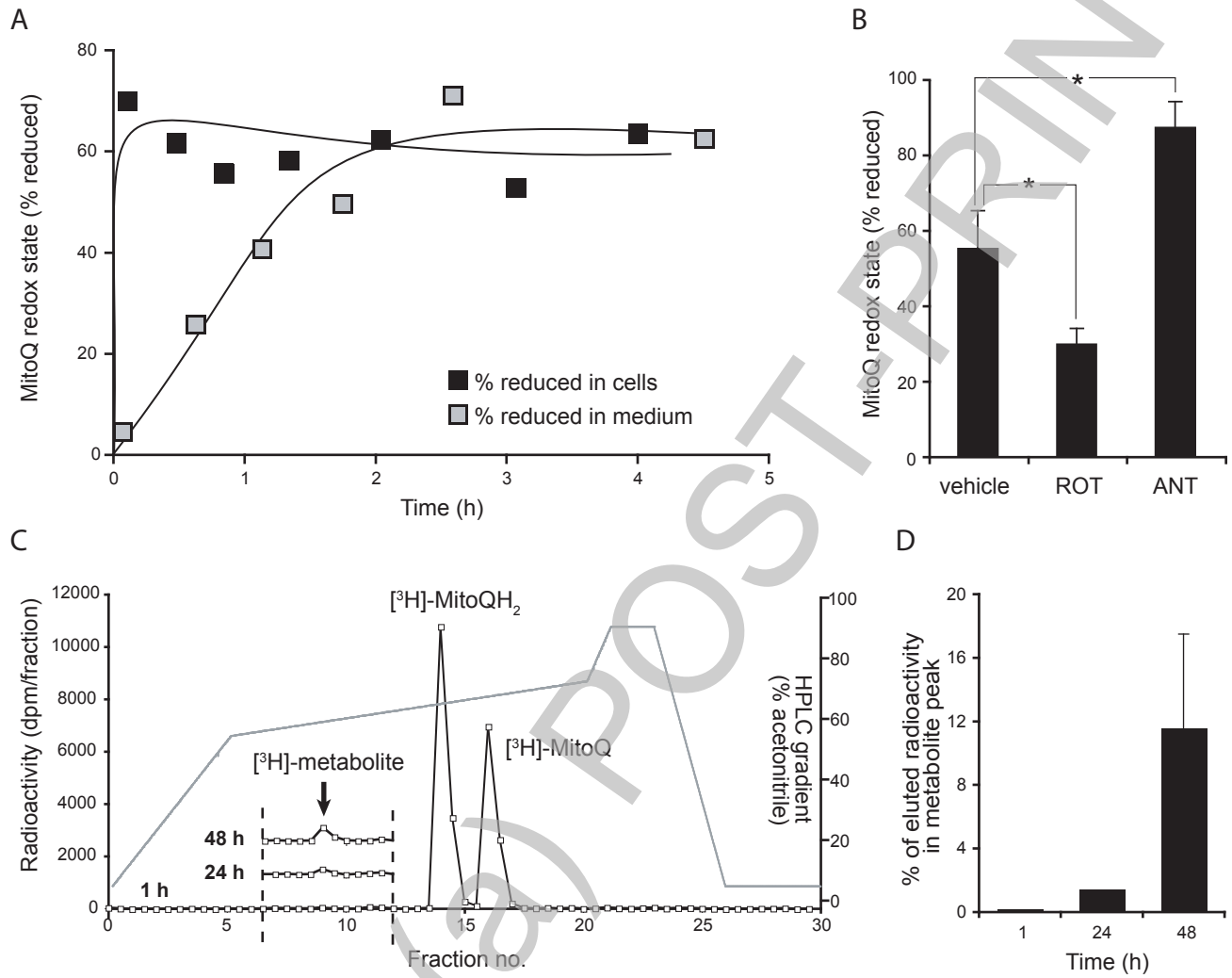


Figure 6



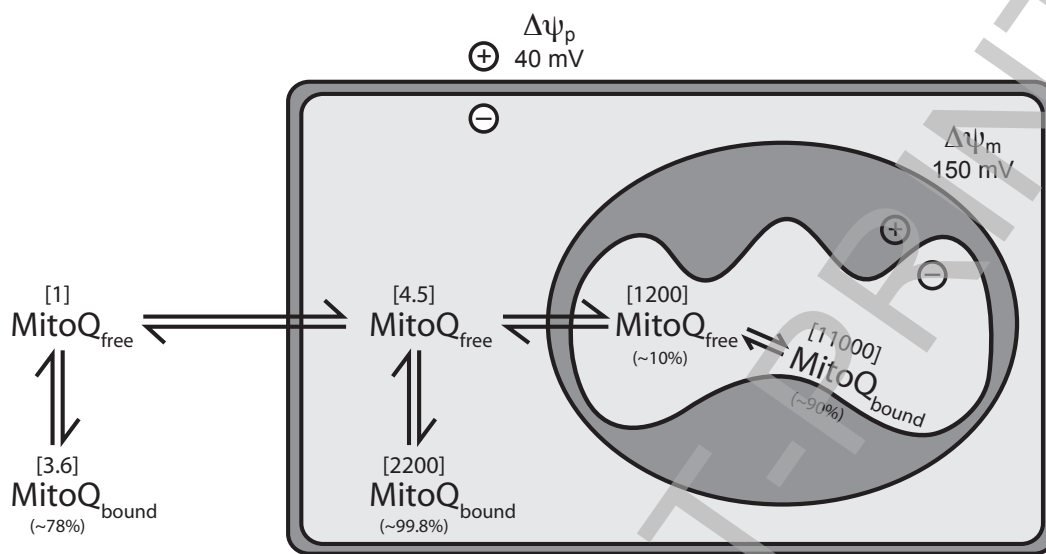
THIS IS NOT THE FINAL VERSION - see doi:10.1042/BJ20080063

Figure 7



THIS IS NOT THE FINAL VERSION - see doi:10.1042/BJ20080063

Figure 8



THIS IS NOT THE FINAL VERSION - see doi:10.1042/BJ20080063

Stage 2(a) POST-PRINT